X-ray standing waves—a new method of studying the structure of crystals

M. V. Koval'chuk and V. G. Kohn

A. V. Shubnikov Institute of Crystallography, Academy of Sciences of the USSR

I. V. Kurchatov Institute of Atomic Energy, Moscow

The physical nature, potentialities, and prospects of application of a new method of studying the structure of crystals and thin surface layers is discussed. It is based on recording secondary radiations such as external and internal photoelectron emission, as well as x-ray fluorescence, under conditions of dynamic x-ray diffraction in single crystals, in which the intensity of the radiation field in the crystal reproduces the periodicity of the crystal lattice in the form of a standing wave along the diffraction vector. The method allows one to measure the absolute displacements of atomic planes in the crystal in fractions of an Angstrom unit, and also to determine the degree of order in the arrangement of atoms in the surface layer. In addition to presenting the history of the problem and reviewing the most important studies published in this field in the past twenty years, the problems of the theory and the experimental technique of the method of standing x-ray waves are presented in considerable detail.

TABLE OF CONTENTS

The standing x-ray wave
Will responsively behave.
It offers immediate reply
On sites that atoms occupy,
And tests the facets of your jewels
For violations of the rules.

1. INTRODUCTION

A new field in the physics of diffraction of hard electromagnetic radiation has arisen and taken shape in the past 20 years. It is based on studying and using standing x-ray waves that arise in a perfect crystal under conditions of dynamic diffraction. Apart from general physical interest involving the anomalously sharp change in the character of the interaction of x-rays with an atom in the crystal, this field, as has now become clear, is highly promising for analyzing the structure of crystals, also at the atomic level.

Actually a standing wave that has the same period as the crystal lattice easily senses the slightest deviation of the atomic planes (or individual atoms) from their correct positions in the ideal crystal. Thus, for example, one can determine the position of impurity atoms implanted in a crystal or the length of a chemical bond for a monolayer of foreign atoms adsorbed on the clear surface of a crystal.

What does a standing x-ray wave amount to? To answer this question, let us examine the propagation of x-rays in a sufficiently thick crystal. Let a plane wave with the wave vector $\mathbf{k}_0$ be incident on the crystal. The propagation of this wave in the crystal is described by Bloch waves, which take into account the translational symmetry of the crystal and amount to a coherent superposition of a refracted and a scattered wave. Their wave vectors are equal to $\mathbf{k}_m = \mathbf{k}_0 + \mathbf{h}_m$, where the $\mathbf{h}_m$ are the reciprocal-lattice vectors of the crystal with the coefficient 2π.

The amplitudes of the scattered waves are determined directly from the Maxwell equations, and are, as a rule, very small—considerably smaller than the amplitude of the refracted wave. This involves the fact that in the x-ray frequency range the dielectric permittivity of the medium $\varepsilon_\mathbf{h}(\omega) = 1 + \chi_\mathbf{h}(\omega)$ differs very little from unit ($\chi_\mathbf{h} \sim 10^{-5}$–$10^{-6}$). Hence the Bloch waves that arise in the crystal almost coincide with the incident plane wave.

However, when certain conditions are satisfied, the situation can change sharply. Thus, if $(\mathbf{k}_0 + \mathbf{h})^2 = k_0^2$ (the Wolf-Bragg condition) for some reciprocal-lattice vector, then the amplitude of the scattered wave bcomes comparable with the amplitude of the refracted wave (the two-wave approximation). In this case, if we neglect the weak scattered

waves, we have the following expression for the amplitude of the electric field in the crystal:

$$E(r) = E_0 e^{ik_0 r} + E_h e^{ik_h r}. \qquad (1)$$

Here we have $k_h = k_0 + h$. The field intensity is determined by the square of the modulus of the amplitude $E(r)$ and equals

$$I(r) = |E_0|^2 \left[1 + \frac{|E_h|^2}{|E_0|^2} + 2\frac{|E_h|}{|E_0|} \cos(hr + \alpha) \right], \qquad (2)$$

Here α is the phase of the ratio (E_h/E_0).

As Eq. 2 implies, the intensity of the wave field in the crystal in this case has a sharply marked spatial dependence in the direction of the reciprocal-lattice vector h. This dependence is periodic, with a period either exactly equal to or smaller by an integer than the interplanar spacing for the system of reflecting planes being studied ($|h| = 2\pi n/d$), while the field intensity is identical on the planes parallel to the reflecting plane of the crystal.

The structure of the standing wave of (2) is determined by two parameters: the ratio $|E_h|/|E_0|$ and the phase α. Depending on the concrete conditions of the experiment, i.e., the deviation of the angle of incidence from the Bragg angle, the geometry of diffraction, the stated parameters can take on different values. For example, let us study the situation in which $|E_h| = |E_0|$, while the phase α varies. Here the maximum value of the intensity exceeds fourfold the field intensity of the reflected wave $|E_0|^2$, while the minimal value is exactly zero.

The mutual arrangement of the atomic planes, i.e., of the maxima of the electron density distribution in the crystal and of the planes of maximum intensity of the wave field, is determined by the value of α. Thus for $\alpha = 0$ the intensity maxima of the field fall on the atom planes, while for $\alpha = -\pi$ the atomic planes coincide with the nodes of the field (Fig. 1). It is quite obvious that in these two limiting cases the nature of the interaction of the field of the x-ray wave with the crystal is sharply different. As will be shown below the situation being discussed is realized in the case of diffraction in the Bragg geometry in the so-called phase-sensitive region of angles of incidence, which corresponds to the region of total reflection of x-rays.

Besides the studied situation, another one exists in which $|E_h| < |E_0|$. In this case a standing wave arises in the crystal as before, but its amplitude, just like its mean value, is
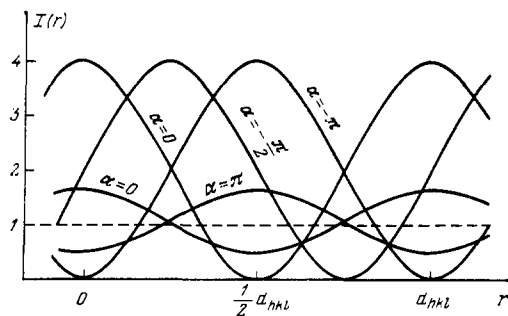

FIG. 1. Intensity distribution of the wave field in a crystal with respect to the atomic planes for different values of $|E_h|/|E_0|$ and the phase α.

smaller than in the previous case. In the limit as $|E_h| \to 0$, which corresponds to a large deviation from the Bragg angle, the amplitude of the oscillations of the standing wave approaches zero, while the mean value becomes equal to the intensity of the plane incident wave (see Fig. 1). In other words a transition occurs from the two-wave to the one-wave approximation.

Thus it becomes clear from what we have said that the character of the interaction of the electromagnetic radiation with the crystal under conditions of dynamic diffraction varies sharply.

An effect involving the existence of a standing wave and the variation of the total field at the atoms forming the crystal lattice has been known for a long time. However, under the conditions of a classical x-ray diffraction experiment that measures separately the intensity of the reflected and the transmitted waves, it is manifested very weakly. This involves the fact that the amplitude of the inelastic scattering channels is considerably smaller than the amplitude of elastic scattering. The standing wave in the crystal manifests itself in a traditional x-ray experiment only in the form of an anomalous angular dependence of the absorption (the anomalous transmission effect in the Laue case, as discovered by Borrmann,[1] and also the weak asymmetry of the diffractive reflection curve in the Bragg case[2,3]).

The most direct and natural method of studying standing x-ray waves and applying them in practice is to record the secondary radiations that arise upon absorption of x-ray quanta. These are primarily photoelectrons and Auger electrons, fluorescence quanta, and thermal diffuse and Compton scattering.

The first step in this direction was taken in 1962 by Batterman,[4] who measured the GeK_α fluorescent radiation in diffraction of MoK_α radiation in a germanium crystal. He used the Bragg diffraction geometry in a two-crystal spectrometer and studied the angular dependence of the fluorescence yield. Despite expectations, the measured curve of the angular dependence proved similar to the inverted reflection curve of the x-rays, and the structure of the wave field manifested itself very weakly only at the edges of the total-reflection region. As will be shown below, the angular dependence of the yield of secondary radiations is determined by the intensity of the wave field at the atoms only when certain conditions are satisfied. Namely, the thickness of the layer emitting the secondary quanta (the escape depth L_{yi}) must be smaller than the minimum depth of penetration of the x-ray radiation (the extinction length L_{ex}). This condition ($L_{yi} < L_{ex}$) specifically was not satisfied in Batterman's experiment.

A completely different situation exists in the case of the external x-ray photoeffect. If fluorescent radiation with the small absorption coefficient μ_{yi} emerges from a sufficiently thick layer of a crystal having the thickness $L_{yi} \approx 1/\mu_{yi}$, then the photoelectrons emerge from a very thin surface layer having a thickness of the order of fractions of a micrometer, which is considerably smaller than the extinction length under ordinary conditions. Even in the first experiments to measure the external photoeffect performed at the beginning of the 1970s at Leningrad University by Efimov, Kruglov,

and Shchemelev,[5-7] it was clearly shown that the angular dependence of the photoemission yield is determined unambiguously by the position of the standing x-ray wave with respect to the atomic planes. Later Golovchenko, Batterman, and Brown[8] found a method for revealing the structure of the wave field by measuring the fluorescence from impurity atoms introduced into the lattice of the crystal matrix at a very small depth. Evidently the condition $L_{yi} < L_{ex}$ is also satisfied here.

In addition to the studies indicated above, studies were conducted as early as the mid-sixties of the angular dependences of the yield of such secondary radiations as thermal diffuse and Compton scattering.[9-11] We note also that the appearance of a standing wave in a crystal gives rise to an anomalous angular dependence of the photo-emf[12,13] and the photoconductivity[14,15] in semiconductor barrier structures.

In the following years the interest in studying the examined processes has grown and expanded. This has led to the rapid development of a fundamentally new experimental technique that considerably simplifies experimentation and makes it faster and more informative. The use of new, powerful radiation sources, such as synchrotron radiation and rotating-anode generators and of fundamentally new systems for stabilizing the angular positioning and rotation of crystals, and computers for processing and accumulating experimental data has converted this field of solid-state physics and surface physics into one of the most current and promising fields.

2. HOW TO SEE AND USE A STANDING X-RAY WAVE

As an introduction to the problem, let us examine the simple situation in which a layer of atoms of a different type exists on the surface of a perfect crystal. For simplicity let us restrict the treatment to the case of symmetrical diffraction in the Bragg geometry, in which the reflected wave emerges from the crystal at the same surface through which the radiation enters the crystal. Evidently such a geometry is preferable for studying the structure of a surface and surface layers, since in this case the x-rays in the range of angles corresponding to total reflection (the so-called phase-sensitive part of the curve) penetrate into the crystal to a small depth, and the thickness of the specimen (contrary to the Laue case) does not affect the structure of the wave field (Fig. 2).

In this case the angular dependence of the ratio of the amplitudes of the fields $|E_h|/|E_0|$ and the phase α for normally polarized radiation (σ-field) has a special form (see, e.g., Refs. 16–22):

$$\frac{|E_h|}{|E_0|} e^{i\alpha} = -(1 - iy_h)^{-1}$$

$$\times \{y - iy_0 + [(y - iy_0)^2 - (1 - iy_h)^2]^{1/2}\} \cdot (3)$$

Here we have

$$y = -\frac{\sin 2\theta_B}{|\chi_{rh}|}(\theta - \theta_0), \quad y_0 = \frac{\chi_{i0}}{|\chi_{rh}|}, \quad y_h = \frac{\chi_{ih}}{|\chi_{rh}|}, \quad (4)$$

θ is the angle of incidence of the x-rays on the crystal, θ_0 is the angle corresponding to the middle of the phase-sensitive region of the reflection curve (the "dynamic" Bragg angle), θ_B is the Bragg angle (kinematic, without allowance for refraction), and χ_{rh}, χ_{i0}, and χ_{ih} are the Fourier components of the real and imaginary parts of the polarizability of the crystal ($\chi = \chi_r + i\chi_i$). For the square root in Eq. (3) one uses the branch having a positive imaginary part.

By using Eqs. (3) and (4), we can easily calculate the angular dependence of the intensity of the wave field by Eq. (2). Figure 3 shows this dependence at the atomic planes (the phase is $\varphi = \mathbf{hr} = 2\pi n$, where n is an integer) for the (220) reflection of CuK$_\alpha$ radiation from a silicon crystal. This same diagram shows the coefficient of reflection for x-rays, which is $|E_h|^2/|E_0|^2$, the phase α, and the interference absorption coefficient μ, which depends on the angle of incidence θ as follows:

$$\mu = \frac{2}{L_{ex}} \text{Re}\,[(1 - iy_h)^2 - (y - iy_0)^2]^{1/2}. \quad (5)$$

Here

$$L_{ex} = \frac{\lambda \sin \theta_B}{\pi |\chi_{rh}|} \quad (6)$$

is the extinction length, while λ is the wavelength of the x-rays. As we see from the diagram, the intensity of the wave field at the atoms varies sharply with varying angle of incidence on the crystal in the central part of the reflection curve, in contrast to the reflection coefficient, which is practically constant in this angular region.

Whereas the reflection amplitude E_h/E_0, being complex, has the phase α, which sharply depends on the angle, as
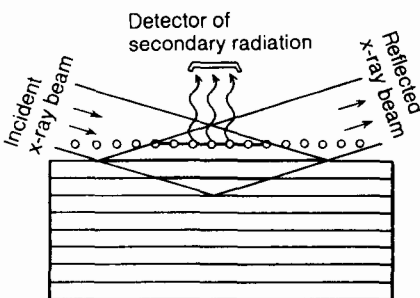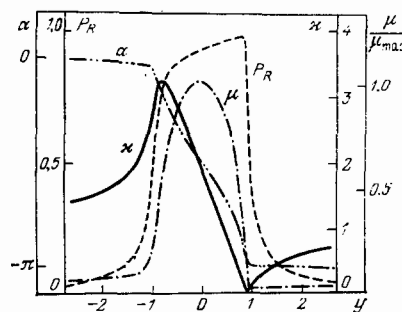

FIG. 2. Diagram of the formation of a standing wave and the escape of secondary radiation from impurity atoms in x-ray diffraction in the Bragg geometry.

FIG. 3. Angular dependences of the intensity of the wave field at the atomic planes ($\varkappa$, solid line), the coefficient of reflection (P_R, dotted line), the interference absorption coefficient (μ, dot-dash line), and the phase α (dash-double-dot line).

we see from Fig. 3, we lose this phase information upon measuring the intensity of the reflected beam, which is proportional to the square of the modulus of the reflection amplitude. On the other hand, the intensity of the wave field at an atom, which is the square of the modulus of the sum of amplitudes of two coherent waves—the refracted wave E_0 and the reflected wave E_h—fixes this phase.

The situation is fully analogous to that which occurs in the holographic method of recording the phase of the scattering amplitude, but here the role of the reference beam in our case is played by the refracted wave. We note also that this opens up a pathway for a direct solution of the phase problem of structure analysis. However, we should recall that we are speaking of a very small range of angles having a magnitude of the order of seconds of angle (0.5×10^{-5} radian). This involves the very small scattering amplitude of x-rays by the unit cell of the crystal, which equal $|\chi_{rh}|$.

Thus we have established that the intensity of the wave field at the atoms of the crystal contains a more complete information. The question naturally arises of how to determine experimentally and use this information. One of the methods of solving this problem consists in measuring the intensity of the yield of secondary radiation, e.g., the characteristic fluorescence from a layer of foreign atoms lying at the surface of the single crystal, which is proportional to the local intensity of the wave field. Let us turn to Fig. 4a. If all the foreign atoms lie strictly in one plane and the position of this plane coincides with the correct position of the reflecting planes in the crystal, then the angular dependence of the yield of fluorescence radiation from these atoms will match the angular dependence of the field intensity shown in Fig. 3.

The actual situation, even as applied to monolayers of atoms adsorbed on the surface of a perfect crystal, can be far more complicated. First, this layer can have any position, which is determined by the length of the chemical bond of these atoms with the atoms of the matrix. Second, it can be somewhat disordered. That is, the atoms forming the layer can deviate randomly from the mean position. Here the overall pattern of all the atoms of the layer are determined by experiment.

Thus, in Fig. 4b the layer in which we are interested is displaced by half the interplanar spacing of the crystal ma-

trix. In this case an additional phase appears in Eq. (2), which equals $P_C = \pi$ in the first order of reflection. This leads to a sharp change in the character of the angular dependence of the fluorescence yield from the impurity atoms, as is clearly shown in the diagram. Actually, whereas the maxima of the field intensity (antinodes) coincide with the position of the atoms in the reflecting planes of the crystal matrix, the position of the layer of impurity atoms corresponds to the field minima (nodes), and vice versa. Hence the curve of the angular dependence (its phase-sensitive part) proves to be a mirror image of the previously discussed ideal case shown in Fig. 4a. Actually the shape of the curve is sensitive to a far smaller displacement of the layers, amounting to small fractions of the interplanar spacing. With a relative experimental accuracy of the order of 1%, one can establish a displacement of the layer of thousandths of the period of the standing wave, which is considerably less than the wavelength of the employed radiation.

A completely different situation arises when the layer of impurity atoms is strongly disordered (Fig. 4c). In this case there are no preferential (coherent) positions of the atoms with respect to the standing wave, and equal fractions of the atoms simultaneously lie both at the antinodes and the nodes of the wave field. Evidently the yield of fluorescence radiation from such a layer is described by Eq. (2) without the third (interference) term, which drops out owing to the averaging over the coordinates of all the atoms of the layer. Here the shape of the curve of the yield of secondary radiation reproduces the shape of the reflection curve of the x-rays and bears no phase information.

The actual pattern is intermediate between the limiting cases that we have discussed. That is, the layer of atoms can be partially disordered and displaced. By performing the statistical averaging of Eq. (2) over the coordinates of all the atoms of the layer, one can easily derive the following expression for the angular dependence of the fluorescence radiation:

$$I = I_0 \left[1 + \frac{|E_h|^2}{|E_0|^2} + 2 \frac{|E_h|}{|E_0|} F_C \cos (P_C + \alpha) \right]. \quad (7)$$

Here we have

$$P_C = \mathbf{h}\mathbf{r}_C = \frac{2\pi n z_C}{d}, \quad (8)$$

$$F_C = \langle \exp [i\mathbf{h}(\mathbf{r} - \mathbf{r}_C)] \rangle = \exp \left(-\frac{1}{2} h^2 \langle (z - z_C)^2 \rangle \right). \quad (9)$$

Here two new parameters have appeared: z_C—the coherent position, i.e., the position of the mean plane of the impurity atoms with respect to the diffraction planes of the crystal, and F_C—the coherent fraction (the Debye-Waller factor), which describes the rms static and thermal displacements of the atoms from the mean position z_C. For simplicity of presentation, below we shall also call the quantity P_C the coherent position. The coordinate z is measured along the normal to the surface of the crystal, which coincides in direction with the diffraction vector $\mathbf{h}$.

Thus, from the experiment discussed above, one can directly measure with high accuracy the coherent position P_C (i.e., the chemical-bond length) and the coherent fraction F_C from the shape of the angular-dependence curve alone.
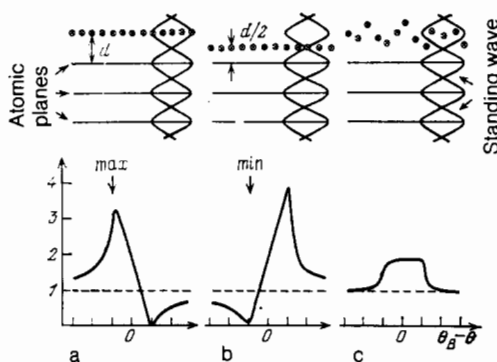

FIG. 4. Diagram illustrating different positions of impurity atoms (circles) with respect to the antinodes of the wave field and the corresponding yield of secondary radiation.
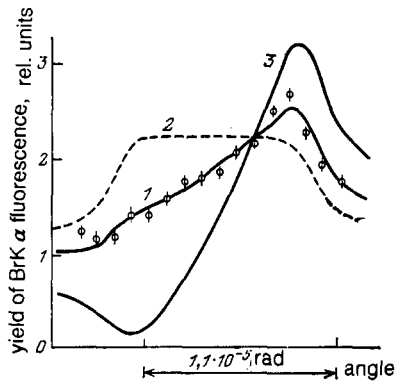
FIG. 5. Angular dependence of the yield of BrK_α fluorescence radiation from a monolayer of Br atoms chemosorbed on a Si surface under conditions of (220) diffraction of MoK_α radiation in Si (curve 1).[23] Curves 2 and 3 correspond to the models of fully disordered and fully ordered layers, respectively.

The thought experiment that we have discussed has been actually performed in the study of Cowan, Golovchenko, and Robbins,[23] who studied the fluorescence of bromine atoms chemosorbed on the surface of a single crystal of silicon by using the (220) reflection of MoK_α radiation. Figure 5 shows the angular dependence of the fluorescence yield obtained by the authors. They determined by processing the experimental data by least squares using Eq. (4) that $F_C = 30\%$, and $z_C = 1.73 \pm 0.07$ Å. This value corresponds to the length of the covalent Si–Br bond.

Actually, as we shall show below, all that we have said in this section on fluorescent radiation is more general in character and pertains to any secondary process having a small escape depth.

3. THE PROBLEM OF EXTINCTION

Now let us examine the yield of secondary radiation excited by a standing x-ray wave from the atoms of the crystal itself. This case is more complicated than the situation already treated for the reason that we must now perform a summation, not only over the coordinates of the atoms lying in one reflecting plane, but also over all reflecting planes that contribute to the measured radiation. In this summation we must take two factors into account. First, the contribution to the overall yield of secondary radiation from atoms lying at different depths in the crystal will differ. This factor is taken into account by using the special function $P(z)$ (the influence function), which determines the weight fraction of the atoms lying at the depth z.

Second, we must take into account the change in the amplitudes of the wave fields $|E_0|$ and $|E_h|$ in the volume of the crystal. In a perfect crystal these amplitudes decline exponentially with increasing depth z, with the rate of decline determined by the interference absorption coefficient μ. In turn, the latter depends on the angle of incidence of the radiation on the crystal (see Fig. 3). Accordingly, we obtain the following expression for the intensity of yield of secondary radiation instead of Eq. (7):

$$I = I_0 \left[1 + \frac{|E_h|^2}{|E_0|^2} + 2 \frac{|E_h|}{|E_0|} F_C \cos(P_C + \alpha) \right]$$

$$\times \int_0^\infty dz P(z) e^{-\mu z}. \tag{10}$$

The concrete form of the influence function $P(z)$ depends on the type of secondary radiation being measured and the conditions of measurement. We shall discuss this function in greater detail below. Here we merely note that in most cases the function $P(z)$ has an exponential form to sufficient accuracy. That is, we have $P(z) = \exp(-z/L_{yi})$, where the parameter L_{yi} characterizes the escape depth of the secondary radiation. Upon substituting this function into Eq. (10) and integrating, we directly obtain

$$I = \frac{I_0}{\mu + \mu_{yi}} \left[1 + \frac{|E_h|^2}{|E_0|^2} + 2 \frac{|E_h|}{|E_0|} F_C \cos(P_C + \alpha) \right], \tag{11}$$

where $\mu_{yi} = 1/L_{yi}$.

Equation (11) differs qualitatively from Eq. (7). Actually, according to (11), the angular dependence of the yield of secondary radiation is now determined both by the magnitude of the local field at the atom and by the thickness of the surface layer contribution to the measured intensity of secondary radiation, which equals $L_{ef} = (\mu + \mu_{yi})^{-1}$. The effective escape depth L_{ef} takes into account also the attenuation of the x-ray wave exciting the secondary radiation, together with the attenuation of the secondary radiation in passing from the depth to the surface of the crystal. Naturally, the actual contribution of the layer at the depth z to the overall radiation yields depends on each of these processes.

Let us again examine the fluorescence radiation, but from the atoms constituting the crystal. As a rule, the escape depth of the fluorescence is large, and often exceeds not only the extinction length L_{ex}, but also even the absorption length L_0 of x-rays far from the region of diffractive reflection. In this case μ_{yi} is considerably smaller than μ, and the effective escape depth L_{ef} is simply equal to the depth of penetration of the x-ray field into the crystal $L = \mu^{-1}$.

Since the depth of penetration of the field into the crystal inside the phase-sensitive range of angles depends on the angle of incidence (see Fig. 3), the angular dependence of the fluorescence yield must acquire a completely different character as compared with the previously discussed case of the yield of radiation from a single plane. In the angular range outside the diffraction region, the fluorescent radiation will emerge from a large volume of the crystal determined by the absorption length L_0. In approaching the center of the angular range of total reflection, the depth of penetration of the field sharply contracts and reaches its minimum value equal to L_{ex}, where L_{ex} is tens of times smaller than L_0. Hence the number of measured quanta of fluorescence radiation declines by a factor of several tens. Against the background of this effect, which is called the extinction effect, the variation of the intensity of secondary radiation owing to the interference character of the formation of the field at the atoms practically vanishes. In other words, the extinction effect makes it impossible to observe the interference behavior of the field, and this means, to obtain phase information.

Actually, one can show upon taking into account Eqs. (3)–(5) that, if the coherent fraction F_C is determined only by the thermal vibrations, i.e., $F_C = y_h/y_0$, then we have

$$L\left(1 + \frac{|E_h|^2}{|E_0|^2} + 2\frac{|E_h|}{|E_0|}F_C\cos\alpha\right) = L_0(1 - P_R). \quad (12)$$

Hence the curve of the yield of secondary radiation has the shape of the inverted reflection curve of the x-rays.

For example, this situation is realized in measuring the fluorescent radiation of GeK_α in a Ge crystal in (220) diffraction of MoK_α radiation. This case has been studied in the pioneer work of Batterman[4] (see also Refs. 24–26). The experimentally measured curve of the angular dependence of the fluorescence yield shown in Fig. 6a practically completely matches the inverted reflection curve, and differs from it only to a very small degree in the "tails" where L_{ef} is not exactly equal to L.

Thus, in the case of secondary radiation with a large escape depth, we face the very serious problem of extinction, which interferes with measuring the standing x-ray wave. To solve this problem one must, on the one hand, decrease the escape depth of the secondary radiation, and on the other hand, increase the depth of penetration of the field into the crystal. However, even for secondary radiation with a large escape depth $L_{yi} \gg L_{ex}$, one can observe the structure of the wave field under the condition $L_{yi} < L_0$ at the edges of the phase-sensitive range of angles. Here, at the edges of this region the effective escape depth L_{ef} is close to L_{yi} and ceases to depend on the angle.

For example, such a case is realized in measuring SiK_α fluorescent radiation under the (220) diffraction conditions

FIG. 6. Experimental curves of the fluorescence yield and reflection under conditions of (220) diffraction of MoK_α radiation for crystals of Ge (a) and Si (b).[26]

of MoK_α radiation in silicon studied in Ref. 26. The experimental curve obtained here is shown in Fig. 6b. We note that all that we have said above holds not only for fluorescence radiation, but also for any other secondary radiation with a large escape depth.

We proceed to analyze the case in which the escape depth of the secondary radiation L_{yi} is smaller than the minimum depth L_{ex} of penetration of the field into the crystal. Naturally, here the effective escape depth L_{ef} practically equals the physical escape depth L_{yi} of the given secondary process, since at the depth L_{yi} the field of the x-ray wave is practically not attenuated. Instead of Eq. (11), we have

$$I = \frac{I_0}{\mu_{y1}}\left[1 + \frac{|E_h|^2}{|E_0|^2} + 2\frac{|E_h|}{|E_0|}F_C\cos(P_C+\alpha)\right]$$
$$\times\left(1 - \frac{\mu}{\mu_{y1}} + \ldots\right). \quad (13)$$

Now the angular dependence of the yield of secondary radiation is mainly determined by the motion of the standing wave through the atomic planes, exactly as in the case with an impurity monolayer, and the effect of extinction plays practically no role.

Equation (13) implies that the maximum change in the shape of the curve owing to extinction arises in this case in the central region. It leads to a weak variation in the slope of the linear region, i.e., to a weak decline in the intensity of the yield at angles θ close to θ_0. We note that in this form the extinction, while actually not distorting the observation of the standing x-ray wave, bears information on the real escape depth of the secondary radiation that can be used in practice.[27,28]

The case being discussed is realized when one measures the external x-ray photoeffect. Precisely because of this circumstance, the external photoeffect has become widely used in studying the structure of surface layers using standing x-ray waves.[29,30]

4. EXPERIMENTAL TECHNIQUE

The experimental measurement of the secondary processes excited by a standing x-ray wave is a relatively complex problem, since one must combine in one instrument the high angular accuracy intrinsic to x-ray diffraction experimentation with the possibility of measuring different inelastic processes, each of which has its own specifics. Naturally, the common feature for all secondary radiations is the use of a multicrystal x-ray spectrometer designed to create the standing x-ray wave in the crystal by realizing the diffraction conditions and to move it over the atomic planes by rotating the crystal past the reflection peak. We note that the problem is that of the high angular accuracy (≈ 0.1 second of angle) required for setting the specimen in the reflecting position, and of the very small angular range (10–100 seconds of angle) corresponding to the region of total reflection of the x-rays. To create a plane x-ray wave experimentally, one uses an asymmetric reflection from one or two crystal monochromators (for more details, see Ref. 31). This is illustrated by Fig. 7, in which the curves are drawn of the yield of photoelectrons from a germanium crystal under conditions of
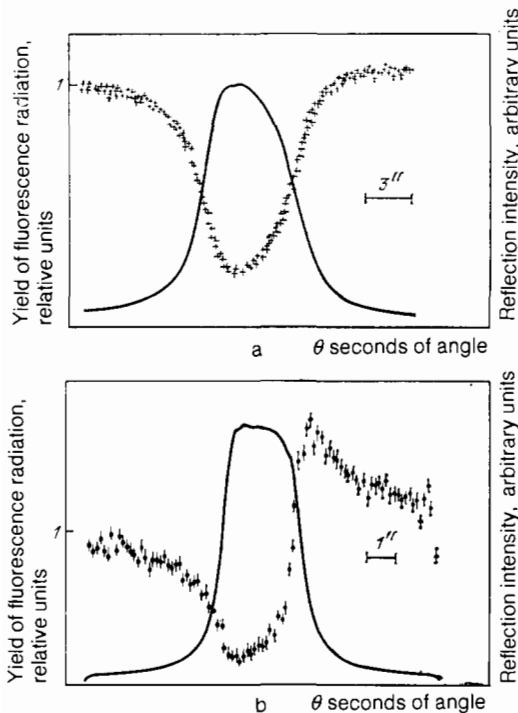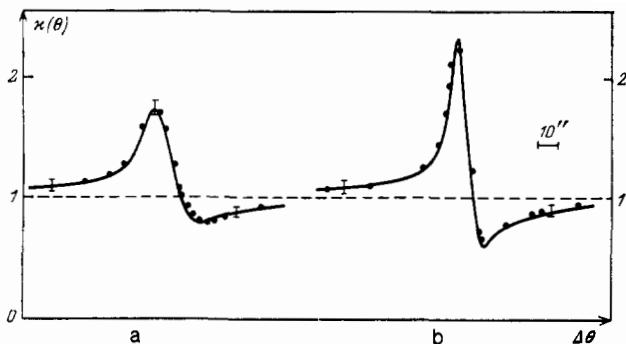
FIG. 7. Angular dependence of photoemission in the case of (111) diffraction of CuK_α radiation in Ge with symmetric (a) and asymmetric (b) monochromators.[53]

FIG. 8. Diagram of an experiment for measuring fluorescence radiation under diffraction conditions.

(111) reflection of CuK_α radiation with symmetric (a) and asymmetric (b) reflection from the monochromator.

Thus the instrumental basis for realizing the standing-wave method is the x-ray spectrometer, which consists of a block of monochromators designed to create the plane incident wave and the precision goniometer employed for adjustment and rotation of the crystal under study. In our country this instrument has been the three-crystal x-ray spectrometer (TXS)[32] developed in the A. V. Shubnikov Institute of Crystallography of the Academy of Sciences of the USSR. The spectrometer must enable making measurements using high orders of reflection (with high values of the Miller indices hkl). This is because the extinction length is increases here (this is important for fulfilling the relationship $L_{yi} \ll L_{ex}$) and the period of the standing wave is decreased, which means that the phase sensitivity of the method is increased.

As regards the specifics of employing high-intensity synchrotron radiation (SR) over a broad energy range,[33] all that we have said above is valid on the whole in this case as well, yet with the difference that the diffraction plane is perpendicular to the plane in which diffraction takes place when one uses ordinary x-ray tubes. Naturally this has required special design solutions—creation of goniometers with horizontally arranged axes of rotation of the crystals. As will be shown below, the use of synchrotron radiation has radically expanded the potentialities of the method of standing x-ray waves by increasing its sensitivity and accuracy, and also by enabling measurements near the absorption edges of the atoms constituting the crystal under study.

We proceed to discuss the experimental aspects of measuring the secondary radiations themselves. To do this one must combine the x-ray spectrometer described above with special attachments that make it possible to measure the secondary radiation with allowance for its concrete specifics.

The situation is simplest of all in which one measures the characteristic fluorescent radiation in the nonvacuum range (wavelength $\lambda < 3$ Å). This requires introducing into the spectrometer only an additional detector besides the scintillation x-ray counter. This detector is set up in the immediate vicinity of the surface of the specimen, and makes it possible to measure fluorescence quanta of the given energy
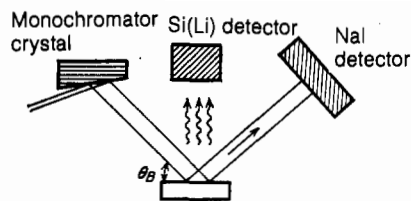
(Fig. 8). For example, it can be a Si(Li) solid-state detector (p-i-n structure), which has an energy resolution of 150–400 eV, and which is used in a complex with a multichannel analyzer.[34]

Apparently this is precisely why the history of employment of standing x-ray waves began with the already mentioned experiment to measure the fluorescence from germanium atoms.[4] We note in passing that, practically immediately after publication of Batterman's study, several articles by Japanese authors[9-11] appeared on the study of Compton and thermal diffuse scattering under diffraction conditions. This is natural, since their measurement requires the same experimental technique as for fluorescence.

The mean free path of photoelectrons in air is very small. Hence their measurement necessarily requires setting up the crystal under study and the detector in a vacuum space. This can be solved in design, either by putting the entire spectrometer in vacuum, as has been done in Refs. 6, 35, and 36, or the specimen under study alone.[37-40] We note that the first experiments to measure photoemission were performed with a total vacuum spectrometer[6] in which even the demountable x-ray tube was situated. This enabled using different wavelengths, including relatively long-wavelength radiation, e.g., CaK_α ($\lambda \approx 3.36$ Å). Owing to their simplicity of design, instruments have become most widespread in which only the crystal and the detector are situated in the vacuum.

The overwhelming majority of the experiments to measure the angular dependence of the yield of photoelectrons performed up to 1980 (apart from several studies by Japanese scientists,[35, 41-44] which will be discussed in detail below) has been integral in type. That is, all the electrons emerging from the crystal were detected, regardless of their energy. In this system of measurements, the SEM (secondary-electron multiplier) detector of photoelectrons in order to increase the number of detected particles was set as close as possible to the surface of the specimen. For the same reason an attractive potential was applied between the specimen and the input of the detector (≈ 200 V). For practical realization of the standing x-ray wave method in the case of integral photoemission, a special vacuum volume has been developed in the form of an attachment to a standard TRS x-ray spectrometer.[45]

The next milestone on the path of development and use of photoemission excited by a standing x-ray wave was the invention of a new vacuum-free method of measurement based on a gas proportional flow-through counter.[46,47] The method is extremely simple and reduces to the idea (by anal-
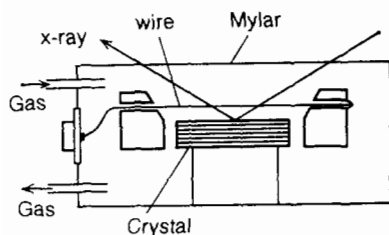
FIG. 9. Schematic diagram of a gas proportional counter.

ogy with the Mössbauer spectroscopy of conversion electrons[48]) that the crystal under study is placed directly inside a gas proportional counter (Fig. 9). The incident x-ray beam enters the counter through a special window covered with a thin organic film (Mylar). On being reflected by the crystal, it exists from the chamber, where it is measured with an ordinary scintillation detector. The electrons excited by the standing x-ray wave in the specimen emerge directly into the gas mixture filling the counter, are accelerated by an electric field created by a high voltage applied between the crystal and a thin filament (electrode), ionize the gas, and are recorded as an electric pulse using a charge-sensitive preamplifier. The gas mixture 90% He + 10% CH_4 has 100% efficiency in detecting electrons and is practically not ionized by x-rays.

The described method has a number of undoubted advantages: simplicity, speed, and the possibility of being realized in any x-ray spectrometer. One can find a detailed description of the operation of the counter and its varieties of design in Refs. 46 and 49–51. Yet the chief merit of the new method is the possibility of distinguishing electrons of a certain energy range (energy analysis). Energy analysis of photo- and Auger electrons excited by a standing wave was first performed[35] by using the already mentioned total-vacuum spectrometer[35,36] fitted with an electrostatic analyzer. This instrument enabled obtaining a number of interesting results with ideal crystals.[41–44] However, it did not become widespread for studying the structure of disturbed layers, apparently because of the small detectable electron yield and certain design features. In a certain sense, it was ahead of its time.

The gas proportional counter as an electron spectrometer of low resolution (≈ 16–20%) has served as the basis for creating a new approach in applying the technique of standing x-ray waves—a depth-selective standing-wave technique intended for layer-wise nondestructive structure analysis based on measuring the angular dependence of the yield of photoelectrons with different energy losses. The idea of layer-wise analysis was first formulated in Ref. 47, while energy-dispersive experiments using a counter were first performed in Refs. 47 and 50–54.

In closing the discussion of the experimental technique of measuring photoelectron emission, we note the recently realized potentiality[55] of performing energy-dispersive measurements by using a magnetic (solenoidal) analyzer. The analyzer amount to a vacuum cylinder arranged horizontally inside the solenoid. The crystal under study, a ring diaphragm, and a secondary-electron multiplier are placed in

the cylinder. By varying the current passed through the solenoid, we vary the magnitude of the magnetic field and thus focus electrons of a certain energy in the detector with a resolution of several percent.

As regards measuring a secondary process such as the internal photoeffect, everything here depends on the choice of method of observing it. For example, in measuring photoconductivity, it suffices to apply to the surface of the studied crystal a thin contact layer of a metal and to connect it to the measuring instrument (electrometer), as was done in the first study of Brümmer and Stephanik to measure photoconductivity in a CdS crystal.[14]

Another method of observing the change in the number of charge carriers (electrons and holes) caused by a standing x-ray wave reduces to measuring the photo-emf that arises in the crystal owing to separation of carriers by the field of a potential barrier in the form of a p-n junction or a Schottky barrier. Actually the potential barrier in this case serves only as an "instrument" that enables seeing the behavior of the wave field. The possibility of measuring the photo-emf was first demonstrated in Ref. 12, while a detailed description of the measurement procedure is given in Ref. 56. To measure the photo-emf, the crystal containing the potential barrier and ohmic contacts is set on a special base having contact joints through an insulating substrate. On the one side, ohmic contacts deposited on regions of the crystal having different types of conduction are connected to these joints, and the measuring instrument on the other side. As one of the variants, one can use a synchronous detector (lock-in amplifier). The entire base is placed in a lightproof cover and is set up in the crystal holder of the x-ray spectrometer. Since the electric signal to be measured is very small (1–$100\,\mu V$), in order to separate it from various parasitic signals, e.g., noise from the contacts, the incident x-rays are modulated with a special modulator rotating with a frequency of several hundred hertz (for more details see Ref. 56).

The entire twenty-year development of the technology of standing x-ray waves, which has been directed toward increasing the sensitivity and accuracy of the method and expanding its potentialities has somehow led to a catastrophic decrease in the measured signal, making it impossible in a number of cases to measure it. For example, the solution of the problem of extinction, which is necessary for isolating the phase-sensitive part of the curve of the angular dependence of the intensity of secondary radiations having a great escape depth ($L_{yi} > L_{ex}$), such as fluorescence and the internal photoeffect (see below) required measuring the weak signal formed by a very thin layer. The same problem arose upon increasing the energy resolution of energy-dispersive measurements of photoemission in the method of the depth-selective technique of standing x-ray waves.

It seemed that the most direct and simple way to solve this problem was to use powerful x-ray sources such as rotating-anode generators and synchrotrons.[57] However, this pathway yields no fundamental solution of the problem, since the application of high-intensity radiation only somewhat shifts the "horizon line". For example, while in an experiment with an ordinary source we can distinguish the fluorescence signal from a certain number of atoms, by using

synchrotron radiation we can decrease this number. However, the next step again requires a new increase in the intensity of the source being used.

The pathway that completely solves the problem of measuring weak signals consists in inventing and using experimentally special accumulation systems, both with ordinary and high-intensity sources.[55, 58-61] We note that the long-time accumulation of a signal under the conditions of x-ray experimentation having high angular accuracy is a very complex problem. The trouble is that one must continuously rotate the studied crystal throughout the entire experiment over a small angular interval (the phase-sensitive region of the curve) in the forward and backward directions so that the angular ranges of each scan coincide to an accuracy of 0.01 seconds of angle.

This is realized by using a piezodrive controlled by dynamic feedback having two loops. One of them serves for linearizing the characteristics of the piezodrive itself by compensating the hysteresis of the piezocrystal by instantaneous measurement of its true elongation (when the control potential has been applied) by using an inductive[55,58] or capacitive[59-61] displacement measuring device. The second loop is intended to enable long-term stability and serves to maintain the curve being measured in the center of the scanning region. This can be easily done, despite the practical lack of the repeated signal of interest to us after one scanning cycle (e.g., in measuring the intensity of the fluorescence yield from a small concentration of impurity atoms), since at the same time we always have a high-intensity reference signal in the form of the diffractive reflection curve of the x-rays.

Using systems of this type enables one to measure with good statistics the signal from a small amount of atoms adsorbed on the surface of a crystal or implanted into its lattice with an ordinary x-ray source.[62] The employment of stabilization systems and synchrotron radiation enables one to reduce the time required for such an experiment from tens of hours to tens of minutes and to reduce the concentration of atoms accessible to study.[63]

5. THEORY

Let us proceed to a more systematic presentation of the theoretical foundations of the technique of standing x-ray waves. As the object of study we shall examine a perfect crystal on which a surface layer of thickness L_d has a distorted structure. These distortions actually can arise upon ion implantation, diffusion of impurity atoms, epitaxial growth, etc., and they vary rather slowly along the surface of the crystal. While neglecting this variation, we shall assume that the distortions are homogeneous along the surface and are characterized by only two parameters: the mean displacement of the atomic planes from their positions in the undisturbed crystal $u(z)$ and the static Debye-Waller factor $\exp(-w(z))$, which depend on the coordinate z along the normal to the surface of the crystal.[64] The amplitude of the overall electric field of the x-rays in the crystal in the two-wave approximation is described by Eq. (1), but with the variable amplitudes E_0 and E_h:

$$E(\mathbf{r}) = \sum_s (\mathbf{e}_{0s}e^{i\mathbf{k}_0\cdot\mathbf{r}}E_{0s}(z) + \mathbf{e}_{hs}e^{i\mathbf{k}_h\cdot\mathbf{r}}E_{hs}(z)). \tag{14}$$

Here $\mathbf{e}_{0s}$ and $\mathbf{e}_{hs}$ are the polarization unit vectors, and $s = \pi, \sigma$.

The scalar amplitudes $E_{0s}(z)$ and $E_{hs}(z)$ satisfy the Takagi-Taupin equations,[65,66] which are derived directly from the Maxwell equations and have the following form in the general case of asymmetric diffraction:

$$\frac{dE_{0s}}{dz} = \frac{i\pi}{\lambda\gamma_0}[\chi_0 E_{0s} + \chi_{\bar{h}}^{(s)}e^{i\varphi(z)-w(z)}E_{hs}],$$

$$\frac{dE_{hs}}{dz} = \frac{i\pi}{\lambda\gamma_h}[(\chi_0 - \alpha)E_{hs} + \chi_h^{(s)}e^{-i\varphi(z)-w(z)}E_{0s}]. \tag{15}$$

Here we have $\varphi(z) = \mathbf{h}\cdot\mathbf{u}(z)$, and γ_0 and γ_h are the cosines of the angles between the vectors $\mathbf{k}_0$ and $\mathbf{k}_h$ and the internal normal to the entrance surface of the crystal $\mathbf{n}_0$. The parameter α characterizes the deviation of the wave vector $\mathbf{k}_0$ from the exact Bragg direction corresponding to the crystal-lattice parameter of the substrate

$$\alpha = \frac{k_h^2 - k_0^2}{k_0^2} \approx -2\sin^2\theta_B\cdot(\theta - \theta_B). \tag{16}$$

The Fourier component of the polarizability tensor of the crystal $\hat{\chi}_0$, $\hat{\chi}_h$, and $\hat{\chi}_{\bar{h}} \equiv \hat{\chi}_{-h}$, being complex, describe both the elastic and the inelastic scattering of x-rays, with $\chi_{\bar{h}}^{(s)} = \mathbf{e}_{hs}\hat{\chi}_h\mathbf{e}_{0s}$ and $\chi_h^{(s)} = \mathbf{e}_{0s}\hat{\chi}_{\bar{h}}\mathbf{e}_{hs}$. The imaginary part of the polarizability tensor $\hat{\chi}_i$ contains contributions from all the inelastic processes: the photoeffect and thermal diffuse and Compton scattering.

To find the intensity of the yield of secondary radiation at the depth z in the crystal, one must determine the number of absorbed quanta in a layer dz thick per unit area and unit time. This can be done most simply by calculating the difference between the input and output fluxes of energy of the x-ray wave in the layer and dividing it by the energy of a quantum of the radiation. This approach was proposed in the study by Afanas'ev and Kon[67] (see also Ref. 68). The corresponding calculation yields the following result:

$$\frac{dN_m^{(s)}(z)}{dz} = \frac{c}{8\pi}\frac{\mu_{0m}}{\hbar\omega}\Bigg[|E_{0s}(z)|^2 + |E_{hs}(z)|^2$$

$$+ 2\,\mathrm{Re}\left\{E_{0s}^*(z)\,E_{hs}(z)\,\frac{\chi_{ih}^{(s)}(m)}{\chi_{i0}(m)}\exp[i\varphi(z) - w(z)]\right\}\Bigg]. \tag{17}$$

Here we have introduced the index m, which characterizes the contribution of a certain (studied) secondary process to the overall amplitudes of inelastic scattering χ_{i0} and $\chi_{ih}^{(s)}$, while we have $\mu_{0m} = 2\pi\chi_{i0}(m)/\lambda$. We recall that the quantities E_{0s} and E_{hs}, being solutions of Eq. (15), depend on the angle of incidence of the x-rays on the crystal.

We obtain the total number of quanta of secondary radiation measured experimentally after integrating Eq. (17) over the coordinate z while taking into account the influence function $P(z)$ introduced in Sec. 3:

$$N_m^{(s)}(\theta) = \int_0^\infty dz\,P_m(z)\,\frac{dN_m^{(s)}(z,\theta)}{dz}. \tag{18}$$

The presented formulas are general. They are valid for any type of secondary radiation including, besides the

photoeffect, fluorescence, thermal diffuse and Compton radiations, also secondary electrons, i.e., Auger electrons and electrons ejected owing to absorption of fluorescence radiation. One must only define appropriately the amplitudes $\chi_{i0}^{(m)}$ and $\chi_{ih}^{(m)}$, as well as the influence function $P_m(z)$.

The Fourier components of the polarizability of a crystal have been calculated in a number of studies in connection with analyzing the anomalous-transmission effect (see, e.g., Refs. 69 and 70). The dielectric permittivity in the x-ray range of frequencies is discussed also in the review of Ref. 71.

According to (17), the number of quanta of secondary radiation is not determined in the general case by the intensity of the wave field at the atoms. Nevertheless, one can write Eq. (17) in a form analogous to Eq. (7):

$$\frac{dN_m^{(s)}}{dz} \sim I_{0s}\left[1 + \frac{|E_{hs}|^2}{|E_{0s}|^2} + 2\frac{|E_{hs}|}{|E_{0s}|}F_C^{(s)}\cos(P_C^{(s)} + \alpha^{(s)})\right].$$

(19)

Here we have introduced the notation

$$I_{0s}(z) = |E_{0s}(z)|^2, \quad \alpha^{(s)}(z) = \arg\frac{E_{hs}(z)}{E_{0s}(z)}$$

(20)

and have omitted the proportionality coefficient.

As Eq. (19) implies, in the most general case the yield of secondary radiation occurs under conditions of formation of the standing x-ray wave in the crystal, while here the coherent fraction

$$F_C^{(s)}(z) = \left|\frac{\chi_{ih}^{(s)}(m)}{\chi_{i0}(m)}\right|e^{-w(z)}$$

(21)

and the coherent position

$$P_C^{(s)}(z) = \varphi(z) + \arg\frac{\chi_{ih}^{(s)}(m)}{\chi_{i0}(m)}$$

(22)

in the disturbed surface layer can depend on the coordinate z.

The simplest case arises in the dipole approximation for the photoeffect and fluorescence in crystals having one type of atoms. For example, for Ge and Si crystals and with reflections with even-even Miller indices, we have

$$F_C^{(s)}(z) = C\exp[-M - w(z)], \quad P_C(z) = \varphi(z).$$

(23)

Here C is a polarization coefficient, which equals unity for σ-polarization and $\cos 2\theta_B$ for π-polarization, and $\exp(-M)$ is the Debye-Waller temperature factor. This case as applied to a perfect crystal and σ polarized radiation has been treated in the previous sections.

For reflections with odd-odd Miller indices the situation becomes somewhat more complicated. Here we have

$$F_C^{(s)}(z) = \frac{C}{\sqrt{2}}\exp[-M - w(z)],$$

$$P_C(z) = \varphi(z) \pm \frac{\pi}{4}.$$

(24)

The sign in front of $\pi/4$ in the formula for P_C depends on the type of reflection. According to (19) and (24), the maximum and minimum yields of secondary radiation are close to the quantity $I_0(2 \pm \sqrt{2})$, and are not equal to zero, even in ideal crystals in diffraction of σ-polarized radiation. This happens because the two sublattices of Ge and Si crystals are projected on the direction of the reciprocal-lattice vector in
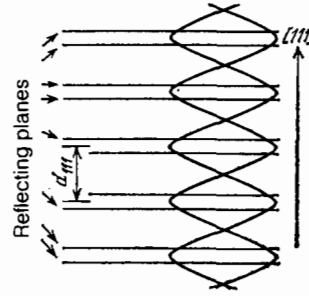

FIG. 10. Diagram illustrating the position of the standing x-ray wave in the case of diffraction at planes with odd-odd Miller indices.

such a way that the projections of the atoms form a periodic chain with a complex basis (Fig. 10). A sinusoidal standing wave cannot be "fitted" to such a chain. In the language of coherent position and fraction this means that the coherent position is found half-way between two close-lying planes (see Fig. 10), while the coherent fraction $F_C \approx 1/\sqrt{2}$ formally describes the deviation of the atomic planes from the coherent position.

An even more complicated situation occurs in noncentrosymmetric crystals, e.g., those consisting of atoms of two types, such as GaAs and InSb, in reflection with odd-odd indices. Here we have

$$\frac{\chi_{ih}^{(s)}}{\chi_{i0}} = C\frac{e^{-M_a} \pm ie^{-M_b}}{e^{-M_a} + e^{-M_b}},$$

(25)

where $\exp(-M_a)$ and $\exp(-M_b)$ are the Debye-Waller temperature factors for atoms of types a and b, while F_C and P_C are found by the general formulas (21) and (22).

We note that an additional possibility appears in this case of spectroscopically distinguishing the secondary radiation from the atoms of only one type (a or b). Then, for the atoms of type a, which lie on the principal sublattice of the crystal, we have

$$F_C^{(s)}(z) = C\exp[-M_a - w(z)],$$

$$P_C(z) = \varphi(z).$$

(26)

For the atoms of type b in the sublattice shifted by one-fourth of the cube diagonal, we obtain

$$F_C^{(s)}(z) = C\exp[-M_b - w(z)],$$

$$P_C(z) = \varphi(z) \pm \frac{\pi}{2}.$$

(27)

According to Eqs. (26) and (27), the atoms of the different types have sharply different coherent positions P_C. Naturally this will lead to a different form of the angular dependence of any secondary radiation in a perfect crystal, under the condition $L_{yi} \ll L_{ex}$. Such a pattern regarding the crystal GaP has been observed in Refs. 44 and 72, and in GaAs crystals in Refs. 73 and 74 (Fig. 11).

Although the dipole term in the multipole expansion of χ_i is the major term, it is not the only one. As the calculations of Wagenfeld, Stephenson, and Hildebrandt[75-77] have shown, the contribution of the quadrupole term amounts to several percent, and must be taken into account in a more exact analysis of the experimental data. Here one must replace the polarization coefficient C in Eqs. (23), (24), (26), and (27) by
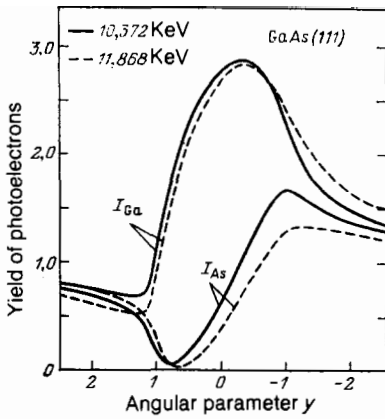
FIG. 11. Angular dependence of the intensity of the wave field in a GaAs crystal at the Ga atoms (I_{Ga}) and As atoms (I_{As}) in (111) diffraction of x-rays with an energy of 10.372 keV (solid line) and 11.868 keV (dotted line) for σ-polarization.[74] The energies of the radiation are chosen to be 5 eV higher than the K-edge of gallium and the K-edge of arsenic, respectively.

$$C_T = (1 - Q)C + QC_1. \qquad (28)$$

Here we have $Q = \sigma^Q / (\sigma^D + \sigma^Q)$ σ^D and σ^Q are the cross-sections for dipole and quadrupole photoabsorption, while the parameter C_1 equals $\cos 2\theta_B$ for σ-polarization and $\cos 4\theta_B$ for π-polarization. In Eq. (25) one must make this substitution separately for the atoms of types a and b:

$$\frac{\chi_{1b}^{(s)}}{\chi_{10}} = \frac{C_T^{(a)} e^{-M_a} \pm i C_T^{(b)} e^{-M_b}}{e^{-M_a} + e^{-M_b}}. \qquad (29)$$

In calculating the dependence of the amplitudes E_{0s} and E_{hs} on z, one need not take into account the weak processes and may restrict the treatment to the dipole approximation as is usually done. The most important effect is diffraction in the Bragg geometry. In this case the solution of Eqs. (15) must satisfy the following boundary conditions: $E_{0s}(0) = E_s^{(in)}, E_{hs}(t) = 0$, where t is the thickness of the crystal. Since the boundary conditions have a rather complicated form, it is convenient to transform to a single nonlinear equation[68] for the quantity

$$R(z) = \frac{E_{hs}(z)}{E_{0s}(z)} \left(\frac{\chi_{\bar{h}}}{\chi_h} \frac{|\gamma_h|}{\gamma_0} \right)^{1/2} e^{i\varphi(z)}. \qquad (30)$$

The latter satisfies the equation

$$\frac{dR}{dz} = \frac{2i}{L_{ex}} [y - iy_0 - Y(z)] R(z) + i \frac{\widetilde{C}}{L_{ex}} e^{-w(z)} [1 + R^2(z)], \qquad (31)$$

where we have

$$\begin{aligned}
& y = -\beta^{1/2} \frac{\sin 2\theta_B}{|\chi_{rh}|} (\theta - \theta_0), \quad \beta = \frac{\gamma_0}{|\gamma_h|}, \\
& y_0 = \frac{\chi_{10}}{|\chi_{rh}|} \frac{1+\beta}{2\beta^{1/2}}, \quad \widetilde{C} = C \frac{(\chi_h \chi_{\bar{h}})^{1/2}}{|\chi_{rh}|}, \\
& Y(z) = -\frac{1}{2} L_{ex} \frac{d\varphi}{dz} = \frac{1}{2} L_{ex} |h_z| \frac{\Delta d(z)}{d}, \\
& L_{ex} = \frac{\lambda (\gamma_0 |\gamma_h|)^{1/2}}{\pi |\chi_{rh}|}.
\end{aligned} \qquad (32)$$

One can solve Eq. (31) taking into account only one boundary condition with $z = t$. If the perfect substrate of the

crystal is thick enough, i.e., $\mu_0 t \gg \gamma_0$, where μ_0 is the normal absorption coefficient, then the solution in the perfect substrate does not depend on the thickness of the crystal. That is, we have $dR /dz = 0$. When we allow for this fact we obtain directly

$$R_0 = \frac{1}{\widetilde{C}} \{y - iy_0 + [(y - iy_0)^2 - \widetilde{C}^2]^{1/2}\}. \qquad (33)$$

Here we employ the branch of the square root having a positive imaginary component. One must solve the equation only in the region $0 < z < L_d$, where L_d is the thickness of the disturbed layer, with the boundary condition $R(L_d) = R_0$.

We obtain the following expression directly from the system (15) for the intensity of the refracted wave:

$$I_0(z) = \exp \left[-\frac{\mu_0 z}{\gamma_0} + \frac{2}{L_{ex}} \text{Im} \left(\widetilde{C} \int_0^z dz' e^{-w(z')} R(z') \right) \right]. \qquad (34)$$

In turn, the curve for diffractive reflection of x-rays is determined by the function

$$P_R^{(s)} = \left| \frac{\chi_h}{\chi_{\bar{h}}} \right| |R(0)|^2. \qquad (35)$$

Equations (15) and (35) completely determine the scheme of calculation of the angular dependence of the yield of secondary processes in the most general case under the condition that a plane wave is incident on the crystal. Actually the experiment is performed in a two-crystal system with a first crystal-monochromator. If one employs asymmetric reflection in both crystals, i.e., the parameter β and the asymmetry factor of the monochromator crystal β_1 do not equal unity, then we have

$$\overline{\varkappa}_m(\varphi) = \frac{N_m(\varphi)}{N_m(\infty)} = \frac{\sum_s \int_{-\infty}^{\infty} dy_1 P_R^{(s)}(y_1) \varkappa_m^{(s)}(y + y_1(\beta_1\beta)^{1/2})}{\sum_s \int_{-\infty}^{\infty} dy_1 P_R^{(s)}(y_1)}. \qquad (36)$$

Here we have

$$y = -\beta^{1/2} \frac{\sin 2\theta_B}{|\chi_{rh}|} (\varphi + \varphi_0),$$

$$\varphi_0 = \frac{|\chi_{r0}|}{\sin 2\theta_B} \left(\frac{1+\beta_1}{2} - \frac{1+\beta}{2\beta} \right), \qquad (37)$$

and φ is the angle between the reflecting planes of the first and second crystals (rocking angle). The function $\overline{P_R}(\varphi)$ is defined analogously.

The presented formalism allows one to analyze theoretically the angular dependence of practically all secondary processes excited by a standing x-ray wave including, besides those mentioned above, the photo-emf and the photocurrent in the Bragg diffraction geometry. The relatively simple situations were treated in the previous sections. In more complex cases for crystals having a disturbed surface layer and an arbitrary relationship between the parameters L_{yi}, L_{ex}, and L_d, one must use a computer to perform the numerical modeling of the experiment and to analyze the experimental data. At present several variants of computation programs have been developed to solve this problem.[68,78,79] The most systematic and universal program as applied to calculating photoemission is described in Ref. 68. It has been effectively used[80] to analyze experimental angular dependences of the
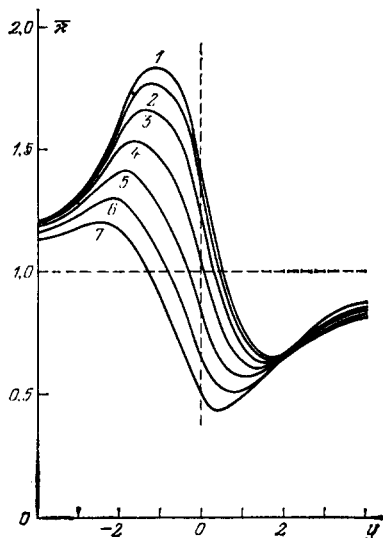
FIG. 12. Angular dependences of the yield of secondary radiation calculated for Si, (400) reflection and CuK_α radiation for different values of the ratio L_{ex}/L_{yi} equal to: 12 (*1*), 7.2 (*2*), 3.6 (*3*), 1.8 (*4*), 0.9 (*5*), 0.45 (*6*), and 0.225 (*7*), in a system with a symmetric monochromator.

external x-ray photoeffect (EXP) from implanted layers on silicon and from epitaxial layers on the surface of germanium and gallium arsenide.

Figures 12 and 13 show examples of the use of the program. Figure 12 presents the calculated angular dependence of the yield of secondary radiation from a perfect Si crystal in the (400) diffraction of CuK_α radiation ($L_{ex} = 3.60\mu$m) in a two-crystal system with a symmetrical monochromator for different values of the parameter L_{yi}. One can see well how the curve varies as the relationship between L_{ex} and L_{yi} varies. Figure 13 shows the results of calculations of the "intrinsic" reflection curves and the EXP in the case of (111) diffraction of CuK_α radiation in a silicon crystal with a

disturbed surface layer. The series of curves corresponds to both the entire layer (upper curves) and to parts of it. The thickness L_d of the layer is comparable with L_{ex}. Hence the change in the shape of the curves is caused both by the change in the coherent position and by the change in the amplitude of the wave fields in the distorted lattice.

A recent study[81] has solved exactly the problem of the angular dependence of secondary processes having an exponential influence function $P(z)$ in a bicrystal, i.e., in a crystal on whose surface a layer exists with an interplanar spacing differing from the matrix and which is partly amorphized. This solution is based on the multilayer algorithm of fast calculation of the curve $\bar{x}(y)$. Combined with the method of fast calculation of the convolution integral using spline interpolation of the curves, a program was developed of automatic processing of the experimental data by least squares (χ^2-fit) in rather complicated situations.

Already today the processing of experimental data obtained by using the standing-wave technique is being performed with computers in a number of studies. Here the signals from the detectors are directly entered into the computer and the output after processing is in the form of values of the concrete parameters of the crystal structure of the crystal under study.

The general theory developed above is valid also for Laue geometry. However, up to now studies in the Laue geometry, both experimental and theoretical, have been performed only on perfect crystals and have been episodic in type.[12-14,56,82-84] The point is that, e.g., in the symmetric Laue case the diffraction vector lies along the surface of the crystal. Therefore the standing wave is also modulated along the surface, and it does not allow one to study the variation of the structure into the interior of the crystal. We note that the study of atomic order in the surface layer along the surface of the crystal is also a highly interesting problem from the physical and applied standpoints, and apparently the
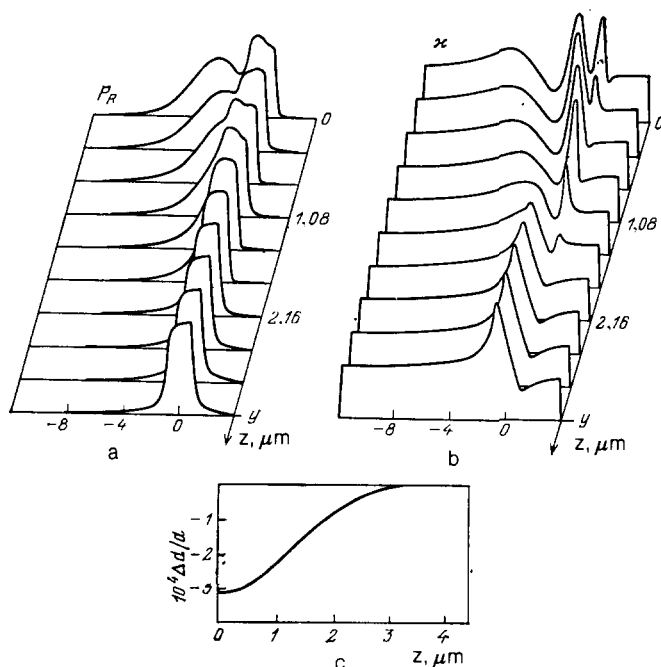

FIG. 13. Curves of the diffractive reflection of x-rays P_R (y) (a) and of photoemission $\varkappa(y)$ (b) calculated for a Si crystal with a perturbed surface layer under conditions of (111) diffraction of a plane monochromatic wave of CuK_α radiation, as well as the dependence of $\Delta d/d$ in the layer on z (c).

scheme of diffraction in Laue geometry will be widely employed in the future in the standing-wave technique. The combination of both diffraction geometries enables one to obtain a two-dimensional pattern of structural distortions in the crystal. The first interesting step in this direction was taken in Ref. 85.

6. PHOTOELECTRIC EMISSION (THE EXTERNAL PHOTOEFFECT)

Let us proceed to a more systematic discussion of the results of studies on the measurement of the external x-ray photoeffect. These studies became most widespread in the first stage, since here the problem of extinction practically does not exist, since the escape depth L_{yi} of the photoelectrons, which usually amounts to fractions of a micrometer, is considerably smaller than the extinction length L_{ex}, which is of the order of several micrometers.

The first studies, which were performed by Shchemelev, Kruglov, et al., were addressed to studying the overall laws of formation of the external photoeffect under x-ray diffraction conditions in perfect crystals. They studied the angular dependence of the photoemission yield in germanium and silicon for different reflections and wavelengths of x-rays.[5–7,86–89]

In analyzing the experimental results, the problem arose directly of the form of the influence function $P(z)$ and the concrete magnitudes of the mean free path of electrons in the crystal. A simple model was proposed[87,88] for the function $P(z)$ based on the following considerations. A photoelectron ejected from an atom undergoes multiple inelastic collisions and rapidly loses its initial direction of motion and energy. This motion in the crystal occurs diffusively. Depending on the value of the initial energy, the electron can pass through a certain distance L_{yi} in the crystal, whereafter its energy has declined to such an extent that it becomes smaller than the work function, and it cannot leave the crystal. In this model the probability of finding the electron above the surface of the crystal is proportional to the area of the surface of a sphere of radius L_{yi} lying above the surface of the crystal.

We can easily convince ourselves that the influence function $P(z)$ in this treatment has the following form:

$$P(z) = \frac{1}{2}\left(1 - \frac{z}{L_{y1}}\right). \tag{38}$$

The parameter L_{yi} is determined experimentally from experiments on transmission of an electron beam of a definite energy through thin films. The book of Bronshteĭn and Fraĭman[90] presents an empirical formula that generalizes the experimental results:

$$L_{y1} = \frac{6 \cdot 10^{-6} AE^{\gamma}}{\rho Z}, \quad \gamma = 1.3 - 1.5. \tag{39}$$

Here ρ is the density of the material in g/cm^3, Z is the atomic number of the element, A is the atomic weight, and E is the initial energy of the electrons in keV. This formula is valid in the energy range E from 0.1 to 10 keV. This model has become widespread in analyzing experimental results in the initial stage of studies.

It was clear practically from the outset that studies on

ideal crystals were purely academic in character, although they allowed one to see explicitly the standing x-ray wave. Naturally, the question arose of the practical application of the method. Evidently, the most suitable object for study by the new method is perfect crystals of semiconductors having a surface layer disturbed by various agents used in the modern technology of solid-state microelectronics (ion implantation, diffusion, laser action, epitaxial growth, and mechanical treatment). The thickness of these layers lies in the range from fractions of a micrometer to several micrometers. Here the study of the structure of these layers using ordinary x-ray diffraction methods proves ineffective owing to the lack of phase information (see, e.g., Refs. 91–94). Moreover, the problem of reconstructing the structure of the disturbed layer from x-ray data alone cannot always be solved unambiguously.[64,94]

As regards the external photoeffect, since the escape depth of the electrons is quite close in order of magnitude to the thickness of these layers, it is most adapted for studying them. Moreover, as we have already mentioned above, the curve of the photoemission yield is highly sensitive to the degree of amorphization (disordering) of these layers, in contrast to the x-ray reflection curve. Therefore the next step in the development involved studying crystals with a disturbed surface layer.

One can provisionally classify these studies into two approaches. The first of these was devoted to studying the displacements of the surface layer at the escape depth of the electrons owing to relaxation of the crystal lattice involving the presence of impurity atoms in the disturbed layer (coherent position). The first study of this series[95] found an anomalous angular dependence of the yield of electrons that sharply differed in shape from the curve for an ideal crystal. A. M. Afanas'ev explained this result on the basis of the hypothesis that the disturbed layer emitting the photoelectrons has atomic planes displaced with respect to their position in the undisturbed part of the crystal by 3/4 interatomic distances. Naturally, by etching part of the disturbed layer one can obtain different displacements of the surface of the crystal, which must explicitly affect the shape of the experimental curves. This idea was fully confirmed in subsequent experiments.[96]

As has already been shown, the phase sensitivity is manifested in purest form when the condition $L_{yi} < L_d < L_{ex}$ is satisfied. The condition $L_d < L_{ex}$ is always satisfied in an ion-doped layer. In order to realize the condition $L_{yi} < L_d$, CaK$_\alpha$ radiation was used in Refs. 95 and 96. As a rule, epitaxial films have a considerably greater thickness $< L_d > L_{yi}$. In this case, to realize the condition $L_{ex} > L_d$, one must use a reflection with high Miller indices. This approach was used in Refs. 38 and 97 in studying epitaxial films of Ge and GaAs [(440) reflection, CuK$_\alpha$ radiation] and also in Refs. 81 and 98 in studying epitaxial films of silicon [(444) reflection, CuK$_\alpha$ radiation].

The second approach involved studying partially or completely disordered layers (coherent fraction).[37,99,100] In one of the studies of this series[100] a simple model was proposed for analyzing the experimental results, in which the

438   Sov. Phys. Usp. 29 (5), May 1986

M. V. Koval'chuk and V. G. Kohn   438

curve of the angular dependence of the yield $\varkappa(\theta)$ is represented as a superposition of two curves: the ideal $\varkappa_{id}(\theta)$ and the curve $\varkappa_a(\theta)$ from a completely amorphous layer, which have fundamentally different and well-known shapes (see Fig. 4):

$$\varkappa(\theta) = K\varkappa_a(\theta) + (1 - K)\varkappa_{id}(\theta). \quad (40)$$

In the case in which the layer being studied is completely amorphized but its thickness L_d is smaller than the escape depth L_{yi} of the electrons, the parameter K evidently characterizes the thickness of the disturbed layer. If, conversely, the thickness of the amorphous layer is known, then one can estimate the escape depth of the electrons by measuring the parameter K experimentally. We note that crystals with an amorphous film of known thickness are a convenient model for studying the process of escape of photoelectrons also in the more complex situation in which the energy loss of the ejected electron is being measured (see below).

Studies have also been performed of photoemission in crystals having the most varied types of disturbances and with an arbitrary relationship between the parameters L_{yi}, L_d, and L_{ex}.[37,80,97] A considerable fraction of these studies has been performed by Zakharov and Sozontov.

The analysis of the experimental data in this case constitutes a more complicated problem and requires introduction of numerical calculations on a computer based on the theory developed in Refs. 67 and 68 (see the previous section). Here the problem can be formulated considerably more broadly, namely, to determine the total profile of the distribution of deformations through the depth of the disturbed layer. Attempts at such a determination based solely on x-ray experimental data have been made by many investigators (see, e.g., Refs. 91–94). However, as the authors of this review have shown,[68] the use of data obtained through two channels, photoemission and x-rays, makes this determination more exact and reliable. A graphic example of this approach is Ref. 80.

In recent years in the technology of microelectronics and surface physics, the attention of investigators has been drawn to ever thinner layers (of thicknesses of the order of hundreds of Ångström units). These layers have also been studied successfully by the method being discussed,[101,102] but naturally the decreased thickness of the layer weakened the contribution of this layer to the measured electron yield. Hence the measurements were performed at the limit of sensitivity. Evidently one can raise the sensitivity of the method by diminishing the total escape depth of the photoelectrons. One of the ways to carry out such a decrease consists in using softer x-rays (as was done in the already mentioned studies of Refs. 95, 96).

Another approach is based on recording the electrons in a certain energy range. As we have already noted above, the first studies along this line on ideal crystals were performed by Japanese scientists, while the studies on specimens with a disturbed layer were performed in the Institute of Crystallography of the Academy of Sciences of the USSR with the participation of one of the present authors (Koval'chuk). In this approach the problem again arises of determining the influence function $P(z,\Delta E)$, which depends on the magni-

tude of the energy losses of the electron as it moves to the surface. This problem is very complicated owing to the complexity of the mechanism of interaction of the electron with the crystal lattice, which is statistical in character.

One of the ways to solve it, which is based on direct numerical modeling by the Monte Carlo method, was developed by Liljequist.[103] In his study the functions $P(z,\Delta E)$ were calculated for different values of ΔE, and also in the integral regime $P(z)$. An approximation by a simple formula was proposed for the function $P(z)$:

$$P(z) = 0.74\left[1 - 2.01\frac{z}{L_{y1}} + 1.02\left(\frac{z}{L_{y1}}\right)^2\right], \quad z < L_{y1}. \quad (41)$$

Here the escape depth L_{yi} is determined by the expression

$$L_{y1} = 780\frac{E^2}{\rho}\frac{1}{\ln(E/E_0)} \quad (\text{Å}). \quad (42)$$

Here the parameters E and ρ have the same meaning as in Eq. (39), while $E_0 \approx 0.39$ keV. Recently Liljequist jointly with the authors of this review have tested Eqs. (41) and (42) by direct calculation by the Monte Carlo method on Si, Ge, and InSb, and have obtained good agreement.

As regards the form of the function $P(z,\Delta E)$ itself, it is nonmonotonic and reaches its maximum value at a certain depth z_{max} that depends on the magnitude of ΔE. Figure 14 shows the schematic form of this function for different values of ΔE. Naturally, the variation of the form of the function $P(z,\Delta E)$ with varying energy of the measured photoelectrons will lead to a variation of the form of the photoemission curve only when the interaction of the standing x-ray wave with the atoms of the crytal is variable (depth-dependent). Such a situation always exists owing to the extinction effect, and also can arise in the presence of distortions that vary at the escape depth. The simplest way to detect this variation consists in using the already mentioned model crystals having an amorphous film of known thickness. This approach was first used in Refs. 27, 28, 50, 52, and 53, and has been developed in Refs. 104 and 105. Moreover, a method has been proposed and realized[105] of determining $P(z)$ from experimental data.

Since the process of propagation of electrons in the crystal described by the function $P(z)$ is general in character for solid-state physics and is employed both in research methods and in technology, the development of methods of direct experimental determination of this function appear important. Apparently this is just why this problem has attracted the attention of investigators in recent years.[84,106,107]
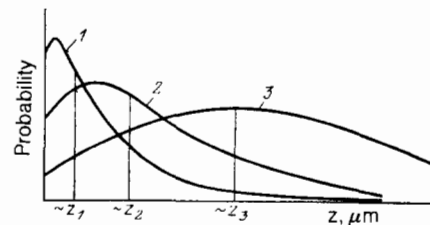

FIG. 14. Schematic diagram of the probability-distribution profiles of escape of electrons with respect to depth for electrons of different energies (curves 1–3).

Observation of a change in the shape of the curves of the yield of photoelectrons caused by an extinction effect is considerably more complicated and requires performing the experiment with high accuracy, since the problem involves very weak changes. Such a unique experiment using synchrotron radiation (with a photon energy of 15.1 keV) and the stabilization system for the angular position of the specimen and a gas proportional counter described above has been performed in Refs. 27 and 28. Figure 15 illustrates the change in the shape of the $\varkappa(\theta)$ curve for an ideal crystal for different electron energies. The processing of these curves enabled determining the mean escape depths. As was expected, the latter increase with increasing magnitude of the energy losses of the electrons.

Actually the use of energy analysis marked the origin of photoelectron spectroscopy excited by a standing x-ray wave, which can be used, e.g., to distinguish the signals from atoms of different types in noncentrosymmetric crystals. The first experimental study of this type was performed by Takahashi and Kikuta[44] on the GaP crystal. They determined the polarity of the faces of the crystal by distinguishing the signal from the GaL electrons with high resolution. We note that measurements on noncentrosymmetric crystals without energy analysis have been performed in Refs. 108–110. Additional potentialities for studies of this type are offered by synchrotron radiation, which allows one to employ any energy range of incident photons of interest to us, including ranges near the absorption edges of one of the elements, when the Fourier component of the polarizability χ (scattering amplitude) for the given element depends sharply on the energy of the incident photon. This leads to a sharp energy dependence of the position of the diffraction planes in the noncentrosymmetric crystal.
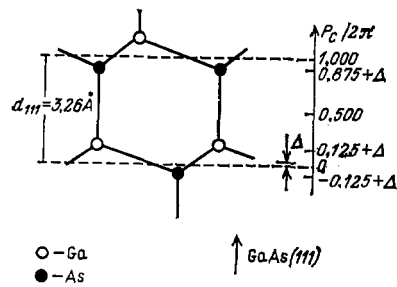
FIG. 16. Diagram illustrating the position of the noncentrosymmetric diffraction planes (111) in a GaAs crystal (dotted lines) with respect to the Ga atoms and the As atoms.[74] The parameter P_C defines the position of the atomic layers in this structure in the (111) direction with respect to the (111) diffraction planes, which are shifted by the amount Δ with respect to the position of the (111) diffraction planes in a centrosymmetric crystal.

This possibility was realized in Ref. 74, in which a small, energy-dependent shift Δ of the diffraction planes amounting to hundredths of an Ångström unit was determined in the noncentrosymmetric crystal GaAs with respect to their position in a centrosymmetric crystal (see Fig. 16). We note in passing that the mean escape depths of electrons in Ge and GaAs crystals and the polarity of the crystal were determined in this same study.

7. FLUORESCENCE RADIATION

The history of the development of the standing-wave technique based on measuring fluorescence radiation amounted in the initial stage to solving the extinction problem. The first step in this direction involved using a detector situated at a small angle to the surface.[24]

Fluorescence quanta emerging from the crystal in directions making an angle of no more than 5° were measured. This experimental geometry enabled a considerable increase in the asymmetry of the "tails" of the phase-sensitive part of the yield curve, but it did not solve the extinctive problem fully.

The next step consisted in using an important specific feature of fluorescence radiation, namely, the easily realizable possibility of high-resolution analysis of the spectral composition of the quanta being detected. This opened up the fundamentally new possibility of measuring the secondary radiation from the atoms of an impurity, either implanted into the lattice of the crystal matrix or deposited on its surface. The first study of this type was performed by Batterman,[25] who measured the fluorescence radiation from arsenic atoms uniformly distributed throughout the bulk of a silicon crystal.

Evidently the situation will be most information-rich in which the impurity is distributed in a thin surface layer. In this case the escape depth is not determined by the mean free path of the fluorescence quanta, but by the thickness of the layer in which the impurity is localized. This directly solves the problem of extinction, and the yield curve has a sharply marked phase-sensitive region. Such a situation has been realized experimentally by Golovchenko et al.[8] by introducing arsenic atoms into silicon to a small depth. This experiment also automatically answered a very important question:
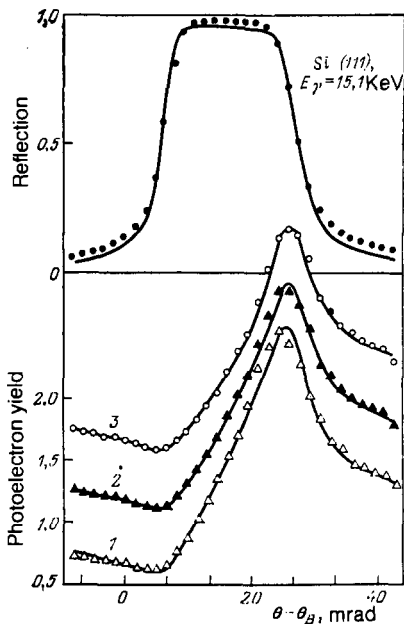

FIG. 15. Angular dependence of the x-ray reflection and the yield of photoelectrons in (111) diffraction of synchrotron radiation with energy of 15.1 keV in a perfect Si crystal.[28] Curves 1–3 correspond to electrons with different energy losses $\Delta E(\Delta E = 0; 2.5;$ and 5 keV, respectively).

where does the impurity lie in the lattice? The shape of the phase-sensitive region of the yield curve obtained in Ref. 8 unambiguously indicated that the arsenic lies at the nodes of the silicon crystal lattice (substitution impurity).

The logical next step was the goal-directed design of an experiment for explicit demonstration of the unique phase sensitivity of the new method. For this purpose Andersen, Golovchenko, and Mair[62] prepared a series of silicon specimens in which arsenic atoms were introduced into a thin surface layer 400-Å thick. Then nitrogen ions were implanted into these specimens to a depth of 2000 Å, with the irradiation dose for different specimens varying from 0 to 5×10^{15} at/cm². Owing to lattice relaxation, the surface layer containing the arsenic atoms proved to be displaced along the normal to the surface, with the magnitude of the displacement depending on the irradiation dose. As was expected, the angular dependences of the yield of AsK_α fluorescence radiation had shapes corresponding to the different values of the coherent position.

This experiment is fully analogous to the experiment that we have already discussed above to measure the external photoeffect, with the sole difference that here the arsenic atoms were used as a "transducer" of a secondary signal with a small escape depth.

We note that, in the course of development of the experimental technique necessary for design of studies of this type (measuring a weak signal), the system was first created for long-term stabilization of the angular position of crystals that was described in Sec. 4. Thus, in Ref. 62 the measurement time amounted to 10 hours. Subsequently, based on the experimental technique invented at Aarhus University (Denmark), broad studies have been conducted on the localization of impurity atoms of different types in silicon single crystals. Then these experiments were continued by Materlik, Hertel, and others by using synchrotron radiation (SR) from the DESY synchrotron (Hamburg, West Germany). This enabled a considerable shortening of the time of experiment (from tens of hours to tens of minutes) and made accessible the measurement of fluorescence from a very small number of impurity atoms (see Ref. 63).

The development of the experimental technique also enabled the start of studies of a fundamentally new type: study of the structural aspects of physical adsorption, chemosorption, etc., i.e., monatomic layers of impurity atoms on the surface of a perfect crystal. This approach was initiated by the study of Cowan, Golovchenko, and Robbins,[23] in which the length of the Si–Br chemical bond was measured (this study has already been discussed in Sec. 2). It was developed in a series of studies using both ordinary sources[111,112] and also SR.[85,113] Let us single out one of the experiments of this type,[114] in which adsorbed layers of Tl and Cd deposited electrolytically on the (111) and (100) surfaces of a single crystal of Cu were studied.

To study the structure of a monatomic layer of Br over a surface, Materlik, Frahm, and Bedzyk[85] were the first to use a standing x-ray wave created in a three-unit x-ray interferometer[115] and varying along the surface (diffraction in the Laue geometry). Instead of measuring the ordinary angular dependence, as had been done in all the experiments that we have discussed thus far, here measurements were simply made of the variation of the fluorescence signal upon uniformly varying the phase in one of the arms of the interferometer, which moved the standing wave along the surface of the crystal.

We return to discussing the studies on fluorescence from atoms of the crystal matrix to note two points. First, for observing an appreciable change in the shape of the curve caused by the phase sensitivity of the yield, the condition $L_{yi} < L_{ex}$ is not so rigid. Thus, for example, one can determine the polarity of the faces of a noncentrosymmetric crystal (GaP)[72] and the siting of the layers of atoms of different types in crystals with a more complex structure, e.g., in gallium gadolinium garnets (GGG)[116] with an escape depth 4–5 times greater than the extinction length L_{ex}.

Second, the relationship $L_{yi} < L_{ex}$ can be satisfied in the case of fluorescence radiation from the atoms of the matrix by a further development of the approach used by Batterman in his first experiment.[24,25] The point is to measure the secondary quanta emerging along the surface of the crystal in a narrow angular range. Thus, Patel and Golovchenko[73] reduced the angular range of collection of the radiation to a magnitude of 7 mrad (as compared with 5° in Batterman's experiment). This required painstaking processing of the surface over a broad area. Figure 17 shows the change in the shape of the curve of GeK_α fluorescence upon a gradual decrease in the collection angle from 34 to 7 mrad. This corresponds to a decrease in the ratio L_{yi}/L_{ex} from 5 to 1 (the escape depth varies here from 1.6 μm to 3000 Å). We see that, even when $L_{yi} = 5L_{ex}$, the shape of the curve is determined to a considerable extent by the motion of the standing x-ray wave over the atomic planes, while upon a further decrease in L_{yi} the influence of the extinction effect practically vanishes. The results being discussed is fully analogous to the previously discussed result of Bedzyk, Koval'chuk, and Materlik[27,28] in which the escape depth was varied by measuring photoelectrons of different energies.

8. THE INTERNAL PHOTOEFFECT

Fundamentally new potentialities are opened up by studying a secondary process such as the internal x-ray photoeffect. The point is to measure the photoconductivity or photo-emf that arises in a semiconductor crystal under x-irradiation under conditions in which a standing wave exists. In contrast to the secondary processes discussed before, in experiments of this type one simultaneously measures both the structural and the electrophysical characteristics of the crystal. In principle this enables us to establish their interconnection.

The history of the development of this approach began in 1968 with the study of Brümmer and Stephanik[14] to measure photoconductivity and the studies of Fokin[12,13] to measure the photo-emf in a crystal having a p-n junction. These studies demonstrated the possibility in principle of observing the anomalous angular dependence of the photocurrent and the photo-emf under diffraction conditions, both in the Bragg and the Laue geometries. The shape of the measured
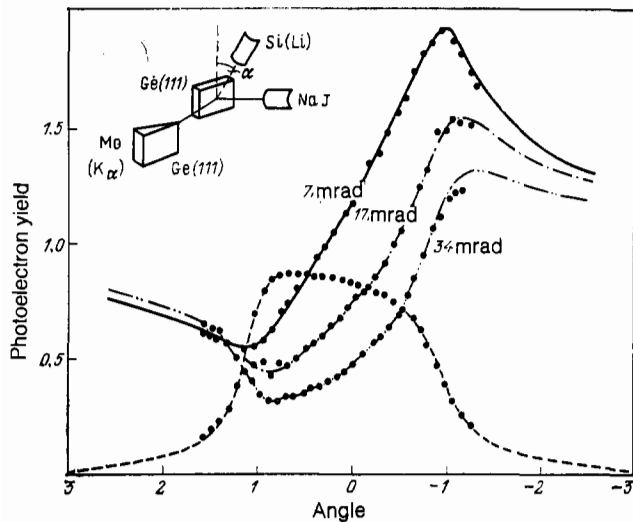
441   Sov. Phys. Usp. **29** (5), May 1986

M. V. Koval'chuk and V. G. Kohn   441

FIG. 17. Angular dependence of the yield of GeK$_\alpha$ fluorescence and of x-ray reflection in (111) diffraction of MoK$_\alpha$ radiation.[73] The fluorescence curves are measured with a Si(Li) detector situated at a glancing angle to the surface, the value of which is indicated in the diagram in milliradians.

curves practically matched the behavior of the angular dependence of the fluorescence yield,[4] which unequivocally indicated the great depth of formation of this process. Starting with this analogy, the statement was made in Ref. 117 that the escape depth in this case is the diffusion length L_D of the minority carriers. These studies were continued in more detail, both theoretically and experimentally, in Ref. 118, in which the correctness of this conclusion was clearly shown.

The cited five studies are the only ones in the past 15 years, which actually indicates the lack of interest in employing this process. This partly involves its small information content arising from the strong effect of extinction. The complication that arises here is fully analogous to that which we discussed in the previous section in treating fluorescence radiation. However, while fluorescence "found its place" in the first stage of solving the extinction problem in studying the position of impurity atoms, no such possibility exists in the case of the internal photoeffect.

Nevertheless, an intensive study has been made in recent years of the specifics of the process, mainly in the Institute of Crystallography of the Academy of Sciences of the USSR. An important study here is that of Zheludeva et al.,[56] where the influence function $P(z)$ was calculated in crystals having a p-n junction, with a thickness of the upper layer $L_{di} > L_{ex}$. The upper layer of the p-n junction under these conditions substantially affects the shaping of the angular dependence of the photo-emf.[119] If we know its thickness, this enables us to determine the diffusion length of the minority carriers in the lower, thicker layer. This conclusion has been graphically confirmed by the results of experimental studies on a series of silicon specimens having different depths of doping of the p-n junction. Detailed theoretical and experimental studies were also performed[56] in the Laue-diffraction case. Here (in contrast to the Bragg case), one must take into account the presence of two Bloch waves in the crystal having different absorption coefficients.

All the studies discussed above were performed on silicon crystals having a large diffusion length ($L_D > L_{ex}$). Just as in the fluorescence case, the natural solution of the extinction problem consists in decreasing L_D. Here the signal of

interest to us decreases, but in contrast to the previous cases, there is no possibility in principle of accumulating it. The use of synchrotron radiation (SR) offers great advantages in this situation.,

Thus, for example, as a rule the diffusion length in GaAs crystals is rather small. In the study of Bedzik et al.,[120] by using SR a photo-emf curve was first obtained in a crystal of gallium[55] arsenide having a Schottky potential barrier with a sharply marked phase-sensitive region (Fig. 18). In addition to the way that we have pointed out, there are other ways to decrease or partially attenuate the effect of extinction. These possibilities have been analyzed by Zheludeva and Koval'chuk[121] with account taken of the specifics of the internal photoeffect, e.g., the potential imparted to the p-n junction. Moreover, as we have already mentioned in analyzing the external photoeffect and fluorescence, in the case in which the angular-dependence curve is only partially distorted by the extinction effect, the effect plays a positive role by bearing information on the specific characteristics of the concrete secondary process. In this case such a characteristic is the diffusion length of the minority carriers, as well as the dimensions of the space-charge region.

A simple and reliable method of weakening the effect of extinction on the shape of the curves is to use high orders of reflection, which lead to increasing L_{ex}, as well as going to
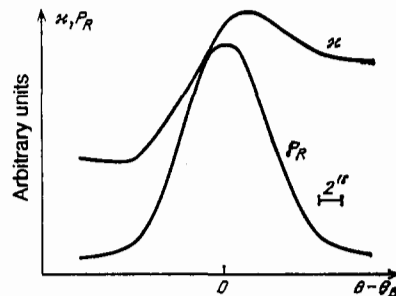

FIG. 18. Angular dependence of the x-ray reflection P_R and the photo-emf $\varkappa$,[120] as measured in the diffraction of synchrotron radiation of energy of 7.74 keV for a Cu/GaAs Schottky barrier and (400) reflection.
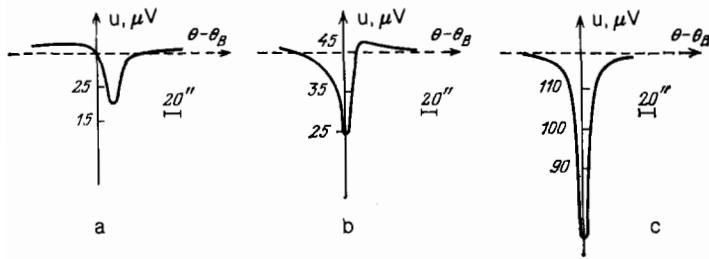
FIG. 19. Angular dependence of the photo-emf in a Si crystal with a *p-n* junction created by diffusion of *P* (initial implantation) (a), and also the curves for the same specimen after annealing for 10 min (b) and 30 min (c). CuK$_\alpha$ radiation, (111) reflection.

x-rays having a large absorption length, which leads to increased asymmetry of the "tails" of the curve.

In closing this section, let us demonstrate the structural sensitivity of the method with the example of measuring the photo-emf in silicon crystals having a *p-n* junction created by diffusional incorporation of phosphorus atoms in a thin surface layer (thickness $\approx 0.2\ \mu$m) (Fig. 19a). Then the specimen was annealed for 10 and 30 min, and the corresponding photo-emf curves were recorded, as shown in Figs. 19b, c. We see the sharp change in the shape of the curve. Let us call attention to the appreciable change in the magnitude of the signal in the angular region far from the center of the region of total reflection. This unequivocally indicates an increase in the diffusion length in the specimens being studied. Generally an important specific feature of this secondary process is the information content of the "background" intensity.

In this regard it is of definite interest to study the angular dependence of the process over a broad range of angles of incidence of the x-rays on the crystal (from 0 to 90°), i.e., the so-called diffraction-free regime. Such a study has been performed in Ref. 122. However, in this study both the experimental results and their interpretation in the region of small (glancing) angles of incidence proved unreliable. A study of this type has been performed more correctly in the already cited study.[56]

9. CONCLUSION

During the decades that have passed since the discovery of x-rays, x-ray diffraction methods have been traditionally employed to obtain structural information on rather large volumes of crystalline solids. This involved the very large depth of formation of the diffraction pattern. This review pictorially reveals that, during the past 10–15 years, x-rays diffraction has been converted into one of the most structure-sensitive methods of studying surfaces. Here we have treated in detail the problems involved in studying standing x-ray waves and using them in practice for analyzing surface layers—a field that has become highly developed at present, being restricted here only to cases of the external and internal photoeffects and also of fluorescence. Actually the potentialities of using standing x-ray waves are somewhat broader. They include the study of thermal diffuse[9–11,123] and Compton[124–127] scattering under conditions of diffraction of the incident radiation, which yields information of a fundamentally new type. Thus, for example, the use of coherent Compton radiation opens a way to determine the nondiagonal elements of the density matrix.[127]

The growing demands of practice, primarily in semiconductor and molecular electronics, and the increased sensitivity of the experimental technique in use have predetermined the intensive development of new x-ray diffraction methods directed toward studying surface structure. They include the so-called two dimensional diffraction, or Bragg diffraction at glancing incidence[128–135] (for more details see the review of Ref. 136) and asymptotic diffraction.[137,138] The increase in surface sensitivity in the first of the cited methods consists in decreasing the thickness of the layer that gives rise to the diffracted wave by decreasing the glancing angle of the x-ray beam incident on the crystal (while maintaining diffraction conditions). In the second case the sensitivity to the surface is based on analyzing the intensity of x-ray reflections separated from the reflection maximum by hundreds of seconds of angle (i.e., the far "tails" of the reflection curve).

In delimiting the spheres the application of these methods and techniques of standing x-ray waves, we note the following. First, these are pure x-ray methods that yields only structural information; for example, asymptotic diffraction yields information only on the mean disorder of the studied layers along the surface. Second, the problem of accumulating the experimental data is complicated in this case by the need to measure a very weak diffracted x-ray beam, in contrast to the situation that arises in the technique of standing waves, where one measures a weak signal of secondary radiation under conditions in which an intense diffracted beam exists. Nevertheless, the use of synchrotron radiation and special high-vacuum apparatus converts glancing-angle diffraction into a delicate method of studying various two-dimensional systems, including monolayers of biological molecules and liquid crystals.[131]

The technique of standing x-ray waves, which is based on measuring the secondary radiations simultaneously with the high-intensity diffracted x-ray beam, has its own specifics and concomitant advantages, the essential one being the possibility of studying thin layers that give rise to a secondary-radiation signal, simultaneously with obtaining structural information about the bulk phase in which diffraction scattering is occurring and the standing x-ray wave is being created. Since the standing wave amounts to a "scale ruler" having a period corresponding to the crystal matrix, in the case of the standing x-ray wave technique (in contrast to the cited pure x-ray methods of surface analysis), there is a unique possibility of determining the position of the surface layer with respect to the crystal lattice of the substrate matrix (e.g., one can determine the chemical-bond length). Moreover, the possibility arises of establishing the interrelationship of the structure with various solid-state properties, in addition to obtaining pure structural information (again a

merit of the standing-wave technique), owing to spectroscopic resolution of the signal from atoms of a certain type.

To a considerable extent, this predetermines the prospects of the development and application of standing x-ray waves.

Thus, in the case of photoelectron emission, the fundamental efforts of investigators in the forthcoming years will be directed toward creating a fundamentally new method—"diffraction x-ray-photoelectron spectroscopy", which amounts to combining the classical high-resolution photoelectron spectroscopy and the technique of standing x-ray waves, as well as the apparatus for realizing it. The realization of this method will enable one to establish the correlation of the electronic properties and structural parameters for atoms forming a surface layer on the basis of analyzing the electron spectra obtained at high resolution and the structural data yielded by the standing x-ray wave.

Marking out the lines of zero characteristic losses for electrons of a certain energy group in a special high-vacuum instrument fitted with means for surface cleaning will enable using a standing x-ray wave for studying structures and various processes (adsorption, desorption, etc.) on atomically clean surfaces of crystals, and also to study (on the atomic level) the initial stages of epitaxial growth, primarily, in the molecular-beam method. Analysis of the different regions of the electrons spectrum lying below the zero-loss line in energy makes it possible to obtain structural information for layers lying at different depths below the surface.

In speaking of the prospects of the internal photoeffect, we note that here one can establish a direct connection between the structural perfection of a semiconductor crystal and its electrophysical properties at depths equal to the diffusion length of the minority carriers, and also can obtain concrete information directly characterizing the space-charge region.

As regards fluorescence radiation, it remains irreplaceable in studying the behavior of impurity atoms, both lying at the surface and implanted into the bulk of solids. We note only the expansion of the number of objects of study that can be had by using fluorescence to study the structure of liquid crystals and Langmuir films.

Special prospects of the standing-wave technique involve using x-ray interferometers.[85] In all the cases that we have treated in this paper, diffraction of x-rays by the crystal (specimen) under study is necessary only as a means for creating a standing wave. This circumstance restricts the present method, since the objects accessible to study include only single crystals or various structures created on their surfaces. The sphere of application of standing waves might be substantially extended by realizing the potentialities of analyzing the structure of the surfaces of amorphous materials, e.g., for studying the process of laser crystallization of the surface of amorphous semiconductors. One can do this by creating a standing wave in space and directing it onto the studied object (like a ray in a microscope). To create the standing x-ray wave one can use an x-ray interferometer, more exactly, the first two blocks of a three-block Laue interferometer. However, here one must solve the problem of the mutual spatial alignment of the specimen under study and the standing x-ray wave.

The further development of the technique of standing x-ray waves doubtlessly involves deepening of our understanding of the features of the coherent interaction of radiation with crystalline matter, the development of the experimental technique, more intensive mastery of synchrotron radiation, and design of physical experiments of a fundamental nature. Here the approach is of especial interest that involves theoretical and experimental study of the specifics of the yield of secondary radiations under conditions of many-wave diffraction, in which the structure of the wave field is substantially more complex than in the two-wave case, since it is simultaneously periodic in two directions. It also seems interesting to design experiments to study secondary radiations under conditions of total internal reflection and diffraction with grazing incidence,[73,139,140] and also with various agents acting on the specimen, e.g., mechanical or thermal. We note that the measurement of the yield of secondary processes over a broad temperature range of the studied crystal is a direct path to determining the mean-square amplitude of the thermal displacements based on data from determining values of coherent fraction.

In perspective, it seems very important to create a new experimental technique that must enable a complex approach to analyzing surface layer and surfaces. Only the employment of the entire set of secondary radiations excited by a standing x-ray wave, combined with the analytical methods now traditional, such as diffraction of slow and fast electrons (LEED and RHEED), electron photo- and Auger spectroscopy, can yield exhaustive information on the structure, composition, and properties of surfaces and thin surface layers of solids and fully solve the problem of characterizing surfaces.

[1]G. Borrmann, Z. Phys. **42**, 157 (1941); **127**, 297 (1950).
[2]M. Renninger, Adv. X-Ray Anal. **10**, 32 (1967).
[3]R. Bubakova, J. Drahokoupil, and A. Fingerland, Czech. J. Phys. Ser. B **12**, 538, 764 (1982).
[4]B. W. Batterman, Appl. Phys. Lett. **1**, 68 (1962).
[5]V. N. Shchemelev, M. V. Kruglov, and V. P. Pronin, Fiz. Tverd. Tela (Leningrad) **12**, 2495 (1970) [Sov. Phys. Solid State **12**, 2005 (1971)].
[6]V. N. Shchemelev and M. V. Kruglov, *ibid*. **14**, 3556 (1972) [Sov. Phys. Solid State **14**, 2988 (1973)].
[7]V. N. Shchemelev, O. N. Efimov, and M. V. Kruglov, Uch. Zap. Leningr. Gos. Univ., No. 370, 83 (1974).
[8]J. A. Golovchenko, B. W. Batterman, and W. L. Brown, Phys. Rev. B **10**, 4239 (1974).
[9]S. Annaka, S. Kikuta, and K. Kohra, J. Phys. Soc. Jpn. **20**, 2093 (1965).
[10]S. Annaka, S. Kikuta, and K. Kohra, *ibid*. **21**, 1559 (1966).
[11]S. Annaka, *ibid*. **24**, 1332 (1968).
[12]A. S. Fokin, Elektron. Tekhn. Ser. 2 "Poluprovodnikovye pribory" (Semiconductor Devices), No. 8 (118), 59 (1977).
[13]A. S. Fokin, *ibid*., No. 8 (126), 30 (1978).
[14]O. Brümmer and H. Stephanik, Phys. Status Solidi A **36**, 617 (1969).
[15]H. Stephanik, Dynamische Interferenztheorie, eds. O. Brümmer and H. Stephanik, Academische Verlag, Leipzig, 1976, p. 181.

[16]W. H. Zachariasen, *Theory of X-Ray Diffraction in Crystals*, Wiley, New York, 1945.

[17]R. W. James, *The Optical Principles of the Diffraction of X-Rays*, rev. ed., Bell, London (1962) (Russ. Transl., Mir, M., 1966).

[18]R. W. James, *Solid State Physics*, eds. F. Seitz and D. Turnbull, Academic Press, New York, 1963, Vol. 15, p. 55.

[19]B. W. Batterman and H. Cole, Rev. Mod. Phys. **36**, 681 (1964).

[20]M. Laue, *Röntgenstrahlinterferenzen*, 3rd edn. (X-Ray Interference), Akademische Verlag, Frankfurt am Main, 1960.

[21]Z. G. Pinsker, *Dynamical Scattering of X-Rays in Crystals*, Springer-Verlag, Berlin, 1978.

[22]Z. G. Pinsker, Rentgenovskaya kristallooptika (X-Ray Crystal Optics), Nauka, M., 1982.

[23]P. L. Cowan, J. A. Golovchenko, and M. F. Robbins, Phys. Rev. Lett. **44**, 1680 (1980).

[24]B. W. Batterman, Phys. Rev. A **133**, 759 (1964).

[25]B. W. Batterman, Phys. Rev. Lett. **22**, 703 (1969).

[26]M. V. Kovalchuk, N. Hertel, M. K. Melkonyan, R. M. Imamov, and P. A. Aleksandrov, Phys. Status Solidi A **66**, K173 (1981).

[27]M. Bedzik, M. V. Koval'chuk, and G. Materlik, Metallofizika **6**, 101 (1984).

[28]M. J. Bedzyk, G. Materlik, and M. V. Kovalchuk, Phys. Rev. B **30**, 4881 (1984).

[29]A. M. Afanas'ev, B. G. Zakharov, R. M. Imamov, M. V. Koval'chuk, and E. F. Lobanovich, Elektron. Prom. No. 11 (95)-12 (96), p. 47 (1980).

[30]B. G. Zakharov, S. S. Strel'chenko, E. A. Sozontov, and M. V. Kruglov, Elektron. Tekhn. Ser. 6 "Materialy", No. 7 (144), p. 46 (1980).

[31]T. Matsushita, S. Kikuta, and K. Kohra, J. Phys. Soc. Jpn. **31**, 1136 (1971).

[32]M. V. Koval'chuk, E. K. Kov'ev, Yu. M. Kozelikhin, A. V. Mirenskiĭ, and Yu. N. Shilin, Prib. Tekh. Eksp. No. 1, 194 (1976).

[33]C. Kunz, ed., *Synchrotron Radiation. Techniques and Applications*, Springer–Verlag, Berlin, 1979 (Russ. Transl., Mir, M., 1981).

[34]R. Woldseth, *X-Ray Energy Spectrometry*, KEVEX Corp., Burlingame, California, 1973 (Russ. Transl., Atomizdat, M., 1977).

[35]S. Kikuta, T. Takahashi, and Y. Tuzi, Phys. Lett. A **50**, 453 (1975).

[36]S. Kikuta, T. Takahashi, Y. Tuzi, and R. Fukudome, Rev. Sci. Instrum. **48**, 1576 (1977).

[37]A. M. Afanas'ev, V. E. Baturin, R. M. Imamov, M. V. Kovalchuk, E. K. Kovev, V. G. Kohn, and S. A. Semiletov, Proc. 7th Int. Vacuum Congress and 3rd Int. Conference on Solid Surface, Vienna, 1977, p. 2209.

[38]E. A. Sozontov, M. V. Kruglov, and B. G. Zakharov, Elektron. Tekhn. Ser. 6 "Materialy", No. 7 (132), p. 108 (1979).

[39]E. K. Kov'ev, E. M. Pashaev, and R. M. Imamov, Prib. Tekh. Eksp. No. 5, 224 (1981).

[40]I. R. Tagirov, V. N. Shchemelev, and S. A. Pauk, Fiz. Tverd. Tela (Leningrad) **23**, 2732 (1981) [Sov. Phys. Solid State **23**, 1601 (1981)].

[41]T. Takahashi and S. Kikuta, J. Phys. Soc. Jpn. **42**, 1433 (1977).

[42]S. Kikuta and T. Takahashi, Jpn. J. Appl. Phys. **17**, Suppl. 17-2, 271 (1978).

[43]T. Takahashi and S. Kikuta, J. Phys. Soc. Jpn. **46**, 1608 (1979).

[44]T. Takahashi and S. Kikuta, *ibid.* **47**, 620 (1979).

[45]M. V. Koval'chuk and Yu. N. Shilin, Elektron. Tekhn. Ser. 6 "Materialy", No. 3 (202), p. 38 (1985).

[46]N. Hertel, M. V. Kovalchuk, A. M. Afanas'ev, and R. M. Imamov, Phys. Lett. A **75**, 501 (1980).

[47]M. V. Koval'chuk, R. M. Imamov, N. N. Faleev, and S. S. Yakimov, Tezisy dokladov Vsesoyuznogo Soveshchaniya po metodam i apparature dlya issledovaniya kogerentnogo vzaimodeĭstviya izlucheniya s veshchestvom (Abstracts of the All-Union Conference on Methods and Apparatus for Studying the Coherent Interaction of Radiation with Matter), Simferopol', 1980, p. 55.

[48]K. R. Swanson and J. J. Spijkerman, J. Appl. Phys. **41**, 3155 (1970).

[49]M. V. Koval'chuk, S. S. Yakimov, R. M. Imamov, N. N. Faleev, Yu. N. Shilin, K. V. Serbinov, and V. Ya. Goncharov, Prib. Tekh. Eksp., No. 6, 185 (1981).

[50]M. V. Koval'chuk and E. Kh. Mukhamedzhanov, Phys. Status Solidi A **81**, 427 (1984).

[51]A. I. Chumakov, A. B. Dubrovin, and G. V. Smirnov, Nucl. Instrum. Methods **216**, 505 (1983).

[52]R. M. Imamov, M. V. Koval'chuk, and E. Kh. Mukhamedzhanov, Tezisy dokladov Vsesoyuznogo Soveshchaniya po metodam i apparature dlya issledovaniya kogerentnogo vzaimodeistviya izlucheniya s veshchestvom (Abstracts of the All-Union Conference on Methods and Apparatus for Studying the Coherent Interaction of Radiation with Matter), Erevan, 1982, p. 106.

[53]M. V. Koval'chuk and É. Kh. Mukhamedzhanov, Fiz. Tverd. Tela (Leningrad) **25**, 3532 (1983) [Sov. Phys. Solid State **25**, 2033 (1983)].

[54]M. J. Bedzyk, G. Materlik, M. V. Koval'chuk, and E. Kh. Mukhamedzhanov, Abstracts VII Intern. Conference on Crystal Growth, Stuttgart, West Germany, 1983, p. SY 5/7.

[55]M. V. Koval'chuk and A. S. Semiletov, Fiz. Tverd. Tela (Leningrad) **27**, 3500 (1985) [*sic*].

[56]S. I. Zheludeva, M. V. Koval'chuk, and V. G. Kohn, J. Phys. C **18**, 2287 (1985).

[57]U. Bonse, X-Ray Sources: Preprint DESY SR-79/29, 1979.

[58]S. K. Andersen, P. K. Bhattacharya, J. A. Golovchenko, N. Hertel, and G. Mair, J. Phys. E **12**, 1063 (1979).

[59]G. L. Miller, R. A. Bone, P. L. Cowan, J. A. Golovchenko, R. W. Kerr, and D. A. H. Robinson, Rev. Sci. Instrum. **50**, 1062 (1979).

[60]A. Krolzig, G. Materlik, and J. Zegenhagen, Nucl. Instrum. Methods **208**, 613 (1983).

[61]A. Krolzig, G. Materlik, M. Swars, and J. Zegenhagen, *ibid.* **219**, 430 (1984).

[62]S. K. Andersen, J. A. Golovchenko, and G. Mair, Phys. Rev. Lett. **37**, 1141 (1976).

[63]G. Materlik and J. Zegenhagen, Phys. Lett. A **104**, 47 (1984).

[64]A. M. Afanas'ev, M. V. Koval'chuk, E. K. Kovev, and V. G. Kohn, Phys. Status Solidi A **42**, 415 (1977).

[65]S. Takagi, Acta Crystallogr. **15**, 1311 (1962).

[66]D. Taupin, Bull. Soc. Franc. Miner. Cryst. **87**, 469 (1964).

[67]A. M. Afanas'ev and V. G. Kohn, Zh. Eksp. Teor. Fiz. **74**, 300 (1978) [Sov. Phys. JETP **47**, 154 (1978)].

[68]V. G. Kohn and M. V. Koval'chuk, Phys. Status Solidi A **64**, 359 (1981).

[69]A. M. Afanas'ev and Yu. Kagan, Acta Crystallogr. A **24**, 163 (1968).

[70]H. Sano, K. Ohtaka, and Y.-H. Ohtsuki, J. Phys. Soc. Jpn. **27**, 1254 (1969).

[71]A. V. Kolpakov, V. A. Bushuev, and R. N. Kuz'min, Usp. Fiz. Nauk **126**, 479 (1978) [Sov. Phys. Usp. **21**, 959 (1978)].

[72]P. Trucano, Phys. Rev. B **13**, 2524 (1976).

[73]J. R. Patel and J. A. Golovchenko, Phys. Rev. Lett. **50**, 1858 (1983).

[74]M. J. Bedzyk, G. Materlik, and M. V. Koval'chuk, Phys. Rev. B **30**, 2453 (1984).

[75]H. Wagenfeld, Phys. Rev. **144**, 216 (1966).

[76]G. Hildebrandt, J. D. Stephenson, and H. Wagenfeld, Z. Naturforsch. Teil A **28**, 588 (1973).

[77]G. Hildebrandt, J. D. Stephenson, and H. Wagenfeld, *ibid.* Teil A **30**, 697 (1975).

[78]Yu. A. Matveev, Fiz. Tverd. Tela (Leningrad) **23**, 51 (1981) [Sov. Phys. Solid State **23**, 28 (1981)].

[79]I. N. Smirnov, A. I. Ponomarev, and V. N. Shchemelev, Fiz. Tekh. Poluprovodn. **18**, 680 (1984) [Sov. Phys. Semicond. **18**, 422 (1984)].

[80]V. G. Kohn, M. V. Koval'chuk, R. M. Imamov, B. G. Zakharov, and E. F. Lobanovich, Phys. Status Solidi A **71**, 603 (1982).

[81]M. V. Koval'chuk, V. G. Kohn, and É. F. Lobanovich, Fiz. Tverd. Tela (Leningrad) **27**, 3379 (1985) [Sov. Phys. Solid State **27**, (1985)].

[82]S. Annaka, J. Phys. Soc. Jpn. **23**, 372 (1967).

[83]A. M. Afanas'ev, R. M. Imamov, A. V. Maslov, and É. M. Pashaev, Dokl. Akad. Nauk SSSR **273**, 609 (1983) [Sov. Phys. Dokl. **28**, 916 (1983)].

[84]A. M. Afanas'ev, R. M. Imamov, and E. Kh. Mukhamedzhanov, Phys. Status Solidi A **83**, K5 (1984).

[85]G. Materlik, A. Frahm, and M. J. Bedzyk, Phys. Rev. Lett. **52**, 441 (1983).

[86]V. N. Shchemelev and M. V. Kruglov, Fiz. Tverd, Tela (Leningrad) **16**, 1472 (1974) [Sov. Phys. Solid State **16**, 942 (1974)].

[87]V. N. Shchemelev and M. V. Kruglov, *ibid.* **17**, 403 (1975) [Sov. Phys. Solid State **17**, 253 (1975)].

[88]V. N. Shchemelev and M. V. Kruglov, Kristallografiya **20**, 251 (1975) [Sov. Phys. Crystallogr. **20**, 153 (1975)].

[89]M. V. Kruglov and V. N. Shchemelev, Fiz. Tverd. Tela (Leningrad) **20**, 2401 (1978) [Sov. Phys. Solid State **20**, 1385 (1978)].

[90]I. M. Bronshteĭn and B. S. Fraĭman, Vtorichnaya élektronnaya émissiya (Secondary Electron Emission), Nauka, M., 1969.

[91]J. Burgeat and D. Taupin, Acta Crystallogr. Sect. A **24**, 99 (1968).

[92]J. Burgeat and H. Colella, J. Appl. Phys. **40**, 3505 (1969).

[93]P. N. Kyutt, P. V. Petrashen, and L. M. Sorokin, Phys. Status Solidi A **60**, 381 (1980).

[94]I. A. Zel'der, R. M. Imamov, M. V. Koval'chuk, and R. S. Senichkina, Elektron. Prom. No. 10 (116)-11 (117), p. 63 (1982).

[95]M. V. Kruglov and V. M. Shchemelev, Materialy vyezdnoĭ sessii

Nauchnogo Soveta AN SSSR po probleme "Obrazovanie i struktura kristallov" (Materials of the Traveling Session of the Scientific Council of the Academy of Sciences of the USSR on the Problem "Formation and Structure of Crystals"), Erevan, 1975, p. 117.

[96]M. V. Kruglov, V. N. Shchemelev, and G. G. Kareva, Phys. Status Solidi A **46**, 343 (1978).

[97]E. A. Sozontov, M. V. Kruglov, and B. G. Zakharov, *ibid.* **66**, 303 (1981).

[98]M. V. Koval'chuk and É. F. Lobanovich, Poverkhnost', No. 5, p. 68 (1984).

[99]M. V. Kruglov, V. N. Shchemelev, B. G. Zakharov, and E. A. Sozontov, Elektron. Tekhn., Ser. 6 "Materialy", No. 10, p. 124 (1975).

[100]M. V. Kruglov, E. A. Sozontov, V. N. Shchemelev, and B. G. Zakharov, Kristallografiya **22**, 693 (1977) [Sov. Phys. Crystallogr. **22**, 397 (1977)].

[101]B. G. Zakharov, M. V. Koval'chuk, Yu. V. Koval'chuk, A. S. Semiletov, O. V. Smol'skiĭ, and E. A. Sozontov, Pis'ma Zh. Tekh. Fiz. **10**, 1402 (1984) [Sov. Tech. Phys. Lett. **10**, 592 (1984)].

[102]E. A. Sozontov, B. G. Zakharov, and V. M. Ustinov, Elektron. Tekhn., Ser. 6 "Materialy", No. 4 (189), p. 35 (1984).

[103]D. Liljequist, Electron Penetration in Solids and Its Applications to Mössbauer Spectroscopy, Preprint, University Stockholm, Inst. Phys., Stockholm, 1979.

[104]A. I. Chumakov, G. V. Smirnov, M. V. Kruglov, and I. K. Solomin, Fiz. Tverd. Tela (Leningrad) **26**, 746 (1984) [Sov. Phys. Solid State **26**, 451 (1984)].

[105]É. Kh. Mukhamedzhanov, A. V. Maslov, A. N. Chuzo, and R. M. Imamov, Poverkhnost', No. 3, p. 54 (1984).

[106]A. V. Maslov and É. Kh. Mukhamedzhanov, Kristallografiya **29**, 408 (1984) [Sov. Phys. Crystallogr. **29**, 246 (1984)].

[107]A. M. Afanas'ev, R. M. Imamov, and É. Kh. Mukhamedzhanov, Fiz. Tverd. Tela (Leningrad) **26**, 1976 (1984) [Sov. Phys. Solid State **26**, (1199) (1984)].

[108]V. N. Shchemelev and M. V. Kruglov, Materialy IV Soveshchaniya po dinamicheskim éffektam rasseyaniya rentgenovskikh lucheĭ i élektronov (Materials of the 4th Conference on Dynamical Effects of X-Rays and Electrons), April 1976, A. F. Ioffe Physicotechnical Institute, Academy of Sciences of the USSR, Leningrad, 1977, p. 178.

[109]I. R. Tagirov, V. N. Shchemelev, and B. G. Zakharov, Zh. Tekh. Fiz., **52**, 815 (1982) [Sov. Phys. Tech. Fiz. **27**, 525 (1982)].

[110]I. R. Tagirov, V. N. Shchemelev, and B. G. Zakharov, Fiz. Tverd. Tela (Leningrad) **24**, 86 (1982) [Sov. Phys. Solid State **24**, 48 (1982)].

[111]M. J. Bedzyk, W. M. Gibson, and J. A. Golovchenko, J. Vac. Sci. Technol. **20**, 634 (1982).

[112]J. A. Golovchenko, J. R. Patel, D. R. Kaplan, P. L. Cowan, and M. J. Bedzyk, Phys. Rev. Lett. **49**, 560 (1982).

[113]J. Zegenhagen, Interner Bericht DESY F41, HASYLAB 84-04, 1984.

[114]G. Materlik, W. Uelhoff, and J. Zegenhagen, Jahresbericht DESY-HASYLAB, 1983, p. 156.

[115]U. Bonse and M. Hart, Appl. Phys. Lett. **6**, 155 (1965).

[116]S. Lagomarsino, F. Scarinci, and A. Tucciarone, Phys. Rev. B **29**, 4859

[117]A. M. Afanas'ev, É. K. Kov'ev, and A. S. Fokin, Pis'ma Zh. Eksp. Teor. Fiz. **28**, 348 (1978) [JETP Lett. **28**, 313 (1978)].

[118]A. M. Afanas'ev, É. A. Manykin, É. F. Lobanovich, M. V. Koval'chuk, and R. M. Imamov, Fiz. Tverd. Tela (Leningrad) **24**, 2599 (1982) [Sov. Phys. Solid State **24**, 1473 (1982)].

[119]S. I. Zheludeva, M. V. Koval'chuk, and S. G. Konnikov, Zh. Tekh. Fiz. **26**, 655 (1984) [Sov. Phys. Tech. Phys. **26**, 395 (1984)].

[120]M. Bedzik, M. V. Koval'chuk, G. Materlik, S. I. Zheludeva, B. G. Zakharov, and P. Funke, Dokl. Akad. Nauk SSSR **282**, 76 (1985). [Sov. Phys. Dokl. **30**, 381 (1985)].

[121]S. I. Zheludeva and M. V. Koval'chuk, Fiz. Tekh. Poluprovodn. **19**, 1597 (1985) [Sov. Phys. Semicond. **19**, 982 (1985)].

[122]É. K. Kov'ev, E. M. Pashaev, A. S. Fokin, R. M. Imamov, and S. A. Semiletov, Elektron. Tekhn. Ser. 2 "Poluprovodnikovye pribory", No. 4 (147), p. 23 (1981).

[123]A. M. Afanas'ev and S. L. Azizian, Acta Crystallogr. Sect. A **37**, 125 (1981).

[124]W. Schülke, Phys. Lett. A **83**, 451 (1981).

[125]J. A. Golovchenko, D. R. Kaplan, B. Kincaid, R. Levesque, A. Meixner, M. F. Robbins, and J. Felsteiner, Phys. Rev. Lett. **46**, 1454 (1981).

[126]W. Schülke, V. Bonse, and S. Mourikis, *ibid.* **47**, 1209 (1981).

[127]W. Schülke, Solid State Commun. **43**, 853 (1982).

[128]W. C. Marra, P. Eisenberger, and A. Y. Cho, J. Appl. Phys. **50**, Part 1, 6927 (1979).

[129]P. Eisenberger and W. C. Marra, Phys. Rev. Lett. **46**, 1081 (1981).

[130]W. C. Marra, P. H. Fuoss, and P. Eisenberger, *ibid.* **49**, 1169 (1982).

[131]I. K. Robinson, *ibid.* **50**, 1145 (1983); Science **221**, 1274 (1983).

[132]A. V. Andreev, É. K. Kov'ev, Yu. A. Matveev, and Yu. V. Ponomarev, Pis'ma Zh. Eksp. Teor. Fiz. **35**, 412 (1982) [JETP. Lett. **35**, 508 (1982)].

[133]A. M. Afanas'ev and M. K. Melkonyan, Acta Crystallogr. Sect. A **39**, 207 (1983).

[134]P. A. Aleksandrov, A. M. Afanas'ev, M. K. Melkonyan, and S. A. Stepanov, Phys. Status Solidi A **81**, 47 (1984).

[135]A. L. Golovin, R. M. Imamov, and S. A. Stepanov, Acta Crystallogr. Sect. A **40**, 225 (1984).

[136]A. V. Andreev, Usp. Fiz. Nauk **145**, 113 (1985) [Sov. Phys. Usp. **28**, 70 (1985)].

[137]S. S. Yakimov, V. A. Chaplanov, A. M. Afanas'ev, P. A. Aleksandrov, R. M. Imamov, and A. L. Lomov, Pis'ma Zh. Eksp. Teor. Fiz. **39**, 3 (1984) [JETP Lett. **39**, 1 (1984)].

[138]A. M. Afanas'ev, P. A. Aleksandrov, R. M. Imamov, A. A. Zavialova, and A. A. Lomov, Acta Crystallogr. Sect. A **40**, 352 (1984)].

[139]P. S. Becker, J. A. Golovchenko, and J. R. Patel, Phys. Rev. Lett. **50**, 153 (1983).

[140]A. M. Afanas'ev, R. M. Imamov, A. V. Maslov, É. M. Pashaev, Kristallografiya **30**, 67 (1985) [Sov. Phys. Crystallogr. **30**, 35 (1985)].

Translated by M. V. King

446   Sov. Phys. Usp. **29** (5), May 1986

M. V. Koval'chuk and V. G. Kohn   446